



PUBLISHED FOR SISSA BY SPRINGER

RECEIVED: July 4, 2012

ACCEPTED: August 30, 2012

PUBLISHED: September 25, 2012

Search for a fermiophobic Higgs boson in pp collisions at $\sqrt{s} = 7$ TeV

The CMS collaboration

ABSTRACT: Combined results are reported from searches for a fermiophobic Higgs boson in the $\gamma\gamma$, WW , and ZZ decay modes in proton-proton collisions at $\sqrt{s} = 7$ TeV. The explored Higgs boson mass range is 110–300 GeV. The data sample corresponds to an integrated luminosity of 4.9–5.1 fb⁻¹. A fermiophobic Higgs boson is excluded at 95% confidence level in the mass range 110–194 GeV, and at 99% confidence level in the mass ranges 110–124.5 GeV, 127–147.5 GeV, and 155–180 GeV.

KEYWORDS: Hadron-Hadron Scattering

JHEP09(2012)111

Contents

1	Introduction	1
2	The CMS detector	2
3	Search channels	3
3.1	Diphoton $\gamma\gamma$ decay mode	3
3.1.1	Dijet tag event class	4
3.1.2	Lepton tag event classes	4
3.1.3	Untagged event classes	5
3.1.4	Signal and background modelling	5
3.1.5	Background modelling in dijet and lepton tag classes	6
3.1.6	Background modelling in the untagged classes	7
3.2	Diboson WW decay mode	9
3.2.1	Dijet tag event class	9
3.2.2	Zero and one-jet event classes	11
3.2.3	Lepton tag event class	11
3.2.4	Signal and background modelling	12
3.3	Diboson ZZ decay mode	12
3.3.1	Signal and background modelling	13
4	Results	13
5	Summary	15
	The CMS collaboration	21

1 Introduction

In the standard model (SM), the electroweak symmetry-breaking takes place through the Higgs mechanism in which a complex scalar doublet with a non-zero vacuum expectation value is introduced and the existence of one scalar particle, the Higgs boson, is predicted [1, 2]. The gauge bosons derive their masses from the additional degrees of freedom gained from the symmetry breaking, and the fermions acquire mass through the direct interaction with the Higgs field itself. It is possible that the mechanism that generates the fermion masses is independent of the Higgs boson. Such a Higgs boson is usually referred to as fermiophobic (FP) [3, 4]. Its decay to W and Z bosons proceeds as in the SM, while the decay to photons proceeds via W loops, i.e. decays to photons via fermion loops are excluded by the model. Since decays to $b\bar{b}$ and $\tau\tau$ are forbidden at tree-level, the branching fraction for a low mass FP Higgs boson ($m_H \approx 120$ GeV) to decay to two vector bosons or two photons is enhanced by an order of magnitude with respect to the SM [5–7]. Previous searches at LEP ([8]; this combination is based on results from the following papers [9–12]), the Tevatron ([13]; this

combination is based on results from the following papers [14, 15]), and the LHC [16] rule out an FP Higgs boson lighter than 121 GeV at 95% confidence level (CL).

In this letter we report on a search for an FP Higgs boson in the mass range 110–300 GeV, in the $\gamma\gamma$, WW , and ZZ decay modes in proton-proton collisions at a centre-of-mass energy of 7 TeV with data collected in 2011 by the Compact Muon Solenoid (CMS) detector at the LHC. The production of the FP Higgs boson is by vector boson fusion (VBF) and associated production with a vector boson (VH). With respect to the SM, the signal is suppressed by an order of magnitude for $m_H > 150$ GeV, is comparable for $m_H \approx 130$ GeV, and is enhanced by an order of magnitude for $m_H \approx 110$ GeV. While for the cases of WW and ZZ the search relies on a re-interpretation of the standard model Higgs boson searches, for the $\gamma\gamma$ final states a dedicated analysis has been put in place. The descriptions of the analyses emphasise the sub-channels and techniques not previously described in recent publications of SM analyses [17–22], namely: the lepton tag and the use of a two-dimensional fit in the $\gamma\gamma$ decay channel, and the lepton tag in the WW decay channel.

2 The CMS detector

While the CMS detector is described in detail elsewhere [23], the key components for this analysis are summarised here.

The central feature of the CMS apparatus is a superconducting solenoid, of 6 m internal diameter, providing a field of 3.8 T. Within the field volume are a silicon pixel and strip tracker, a crystal electromagnetic calorimeter (ECAL) and a brass/scintillator hadron calorimeter (HCAL). Muons are measured in gas-ionisation detectors embedded in the steel return yoke. Extensive forward calorimetry complements the coverage provided by the barrel and endcap detectors.

The inner tracker measures charged particles within the pseudorapidity range $|\eta| < 2.5$. It consists of 1440 silicon pixel and 15 148 silicon strip detector modules.

The ECAL consists of two parts: the barrel which covers the pseudorapidity η range $|\eta| < 1.48$, and the endcaps covering the range $1.48 < |\eta| < 3.0$, where $\eta = -\ln[\tan(\theta/2)]$, and θ is the polar angle of the anticlockwise trajectory of a particle with respect to the beam direction. When used for detector positions the trajectory is assumed to originate at the nominal interaction point, corresponding to the coordinate system origin. The ECAL consists of lead tungstate crystals arranged in a quasi-projective geometry. In the barrel region the front face of the crystal is approximately 22×22 mm², corresponding to a granularity of $\Delta\eta \times \Delta\phi = 0.0174 \times 0.0174$. In the endcap the front face of the crystals is approximately 29×29 mm².

In the region $|\eta| < 1.74$, the HCAL cells have a granularity of $\Delta\eta \times \Delta\phi = 0.087 \times 0.087$, and for $|\eta| < 1.48$, map onto arrays of 5×5 crystals in ECAL to form calorimeter towers projecting radially outwards from the nominal interaction point. At larger values of $|\eta|$, the size of the towers increases and the matching ECAL arrays contain fewer crystals. Within each tower, the energy deposits in ECAL and HCAL cells are summed to define the calorimeter tower energies, subsequently used to provide the energies and directions of hadronic jets. A quartz-fibre Cherenkov calorimeter extends the coverage to $|\eta| < 5.0$.

3 Search channels

The search is performed using three decay modes of the FP Higgs boson. In the analysis of the $\gamma\gamma$ and the WW decay modes, characteristic signatures of FP Higgs boson production via VBF and VH are exploited to select events and suppress background: the two forward jets produced by the scattered quarks in VBF production (dijet tag) and isolated charged leptons (electrons or muons) from decays of the vector bosons in VH production (lepton tag).

In the $\gamma\gamma$ decay mode, events with two isolated and high transverse momentum (p_T) photons are selected. Seven event classes are defined: three of diphoton events which additionally require at least a pair of jets, an isolated muon, or an isolated electron, respectively, and four comprising the remaining diphoton events which are subdivided according to the photon shower shape and position in the detector [17].

In the WW decay channels, the events are characterised by the presence of two opposite sign, isolated high p_T leptons from the W decay, together with large missing transverse energy (E_T^{miss}) due to undetected neutrinos. One sub-channel is defined by additionally requiring the presence of two jets with the VBF topology [18], and another by requiring the presence of a third isolated, high p_T lepton. The selection requiring a third lepton is intended to select Higgs boson production in association with a W boson (WH). Final states with one or zero jets, each separated into events where the leptons have the same flavour and those where there is an electron and a muon, add a further four WW sub-channels, giving a total of six.

In the case of the ZZ final state, production mode signatures are not exploited, and the results of SM Higgs searches [19–22], comprising 19 sub-channels, are simply re-interpreted from the different signal rates expected in an FP Higgs boson model.

The final result is obtained from the combination of 32 mutually exclusive sub-channels from the three decay modes, $\gamma\gamma$, WW , ZZ , as summarised in table 1. The luminosity calculation for the datasets used has been updated with respect to that used in the SM Higgs production analysis of the same channels, published in the references given in the table.

The cross sections for the Higgs boson production mechanisms and decay branching fractions, together with their uncertainties, are taken from ref. [24] and are derived from refs. [25–30]. The VBF production of the FP Higgs boson signal is simulated using the next-to-leading order matrix element generator POWHEG 1.0 interfaced with PYTHIA 6.4.24 [31] for parton showering and fragmentation. The VH signal production channel is simulated with PYTHIA. Samples of Monte Carlo (MC) simulated events used in the analysis are passed through the GEANT4 [32] model of the CMS detector and reconstructed with the same software as used for collision data.

3.1 Diphoton $\gamma\gamma$ decay mode

In the $\gamma\gamma$ channel [17], two isolated photon candidates are required to be within the ECAL fiducial region $|\eta| < 2.5$, excluding the barrel-endcap transition region $1.44 < |\eta| < 1.57$. The shape of electromagnetic shower is used to identify photons, while track veto is used to exclude electrons. Isolation is used to reject the background due to electromagnetic showers

Channel	m_H range (GeV)	Sub- channels	Luminosity (fb^{-1})	Reference
$H \rightarrow \gamma\gamma$	110–150	4	5.1	[17]
$H \rightarrow \gamma\gamma + \text{dijet}$	110–150	1	5.1	[17]
$H \rightarrow \gamma\gamma + \text{lepton}$	110–150	2	5.1	
$H \rightarrow WW \rightarrow 2\ell 2\nu$	110–300	4	4.9	[18]
$H \rightarrow WW \rightarrow 2\ell 2\nu + \text{dijet}$	110–300	1	4.9	[18]
$H \rightarrow WW \rightarrow 2\ell 2\nu + \text{lepton}$	110–300	1	4.9	
$H \rightarrow ZZ \rightarrow 4\ell$	110–300	3	5.0	[19]
$H \rightarrow ZZ \rightarrow 2\ell 2\nu$	250–300	2	5.0	[20]
$H \rightarrow ZZ \rightarrow 2\ell 2q$	130–165, 200–300	6	5.0	[21]
$H \rightarrow ZZ \rightarrow 2\ell 2\tau$	180–300	8	5.0	[22]

Table 1. Summary of analysis channels and sub-channels included in the combination.

originating in jets — mainly due to single and multiple π^0 s [17]. The isolation requirements are applied as a constant fraction of the candidate photon p_T , effectively cutting harder on low p_T photons. The R_9 variable, defined as the energy sum of 3x3 crystals centred on the crystal with maximum energy deposit divided by the total clustered energy, is used to distinguish photons of well measured energy.

3.1.1 Dijet tag event class

Candidate diphoton events for the dijet-tagged channel have the same selection requirements as in the SM search [17]. In the events from the VBF production, the p_T of the Higgs boson is boosted giving enhanced asymmetries in the photon pair energies and hence favoring a lower threshold on one of the two photons. The threshold requirements for this class are $p_T^\gamma(1) > 55 \times m_{\gamma\gamma}/120$, and $p_T^\gamma(2) > 25 \text{ GeV}$.

For each event, hadronic jets are clustered from the reconstructed particles with the infrared and collinear safe anti- k_t algorithm [33], operated with a size parameter R of 0.5. The selection variables for the jets use the two highest p_T jets in the event with pseudorapidity $|\eta| < 4.7$. The selection requirements are optimised to obtain the best expected limit at 95% CL on the VBF signal cross section with fully simulated VBF signal events and the diphoton background estimation from data [17]. The p_T thresholds for the two jets are 30 and 20 GeV, and the pseudorapidity separation between them is required to be greater than 3.5. The dijet mass is required to be greater than 350 GeV. Two selection criteria, relating the dijet to the diphoton system, are applied: the difference between the average pseudorapidity of the two jets and the pseudorapidity of the diphoton system is required to be less than 2.5 [34], and the difference in azimuthal angle between the diphoton system and the dijet system is required to be greater than 2.6 radians.

3.1.2 Lepton tag event classes

Candidate diphoton events for the lepton-tagged channel have the same selection requirements imposed on the photons as in the SM search [17] except for the p_T thresholds. As it

is the case in the VBF, the p_T of the Higgs boson is also boosted in the VH production. To maximize the signal efficiency, the photon p_T thresholds are set to $p_T^\gamma(1) > 45 \times m_{\gamma\gamma}/120$, and $p_T^\gamma(2) > 25$ GeV.

The lepton tag requires at least one muon or electron with $p_T > 20$ GeV, within $|\eta| < 2.4$ for muons, and $|\eta| < 2.5$ for electrons. Electrons are identified as a primary charged particle track and one or more ECAL energy clusters corresponding to this track extrapolation to the ECAL and to possible bremsstrahlung photons emitted along the way through the tracker material. Muons are identified as a track in the central tracker consistent with either a track or several hits in the muon system, not associated with a significant energy deposit in the calorimeters.

The leptons are required to be isolated, using isolation criteria similar to those used for photons [17], and to be separated from the photons by $\Delta R > 1$, where $\Delta R = \sqrt{\Delta\eta^2 + \Delta\phi^2}$. To protect against the background events that arise from an electron misidentified as a photon in the SM process $Z \rightarrow ee$, it is required that the mass of the photon-electron system is not within ± 5 GeV of the nominal Z boson mass.

3.1.3 Untagged event classes

A substantial fraction of the $H \rightarrow \gamma\gamma$ signal events are not expected to pass either the dijet or lepton tag. A statistically independent search is performed on untagged events by using diphoton events that pass the $\gamma\gamma$ selection, and photon p_T requirements of $p_T^\gamma(1) > m_{\gamma\gamma}/3$ and $p_T^\gamma(2) > m_{\gamma\gamma}/4$, but do not pass the selection for either of the two tagged channels. Higgs bosons produced by VBF and VH mechanism have a harder transverse momentum spectrum than those of the photon pairs produced by the background processes [35], and thus the background can be rejected while retaining high signal efficiency, by placing a requirement on the transverse momentum of the diphoton pair, $p_T^{\gamma\gamma}$. It is required that $\pi_T^{\gamma\gamma} \equiv p_T^{\gamma\gamma}/m_{\gamma\gamma} > 0.1$.

The selected events are divided into four classes according to the expected mass resolution and amount of background contamination [17]. Two photon classifiers are used: the minimum R_9 of the two photons, R_9^{\min} , and the maximum absolute pseudorapidity of the two photons. The class boundary values for R_9 and pseudorapidity are chosen to match those used to categorise photon candidates for photon identification cuts. The untagged diphoton event classes are: (a) both photons in barrel and $R_9^{\min} > 0.94$, (b) both photons in barrel and $R_9^{\min} < 0.94$, (c) one or both photons in endcap and $R_9^{\min} > 0.94$, and (d) one or both photons in endcap and $R_9^{\min} < 0.94$.

The numbers of events in the $\gamma\gamma$ sub-channels are shown in table 2, for simulated signal events and for data. A Higgs boson with $m_H = 120$ GeV is chosen for the signal, and the data are counted in the mass range 100-180 GeV. The table also shows the mass resolution, σ_{eff} , defined as half the width of the narrowest window containing 68.3% of the distribution.

3.1.4 Signal and background modelling

In the SM $H \rightarrow \gamma\gamma$ analysis [17], the diphoton mass spectrum of the signal and background are assumed to be described by analytical functions. The signal shape was determined

	Dijet tag	Lepton tag	Untagged			
			(a)	(b)	(c)	(d)
Data ($100 < m_{\gamma\gamma} < 180$ GeV)	122	9	3866	5496	3043	4201
Signal ($m_H = 120$ GeV)	21.8	4.4	23.1	23.9	10.1	11.5
Expected bkg ($115 < m_{\gamma\gamma} < 125$ GeV)	21.2	1.3	678.5	985.2	537.5	754.3
σ_{eff} (GeV)	1.67	1.63	1.19	1.70	2.54	2.94

Table 2. Number of selected events in the $\gamma\gamma$ event classes, for data in the mass range 100–180 GeV and for an FP Higgs boson signal ($m_H = 120$ GeV). The expected number of background events in the signal region 115–125 GeV obtained from the background fit and the mass resolution for the 120 GeV FP Higgs boson signal in each event class are also given.

from the Z to electron mass spectrum, while the background was described by smoothly falling analytical functions of various forms. In this analysis an additional observable based on the diphoton transverse momentum, $\pi_T^{\gamma\gamma}$, is used to construct two-dimensional (2D) probability distribution function (PDF) for the four untagged event classes. This enables further exploitation of the difference between the signal and background diphoton transverse momentum spectra. Z boson decays to electrons are used to derive the amount of additional smearing that needs to be applied to photons in MC simulated events to reproduce the energy resolution observed in the data. These smearing corrections are between 0.7 and 3%, derived for photons separated into four η regions (two in the barrel and two in the endcap) and two categories of R_θ . The uncertainties on these corrections and factors accounting for the difference between photons and electrons are taken as systematic errors in the limit setting procedure.

The signal mass PDF, $\mathcal{M}_s(m_{\gamma\gamma})$, is extracted, after the smearing, by parameterising the $m_{\gamma\gamma}$ distribution in simulated signal events with a sum of Crystal Ball [36] and Gaussian functions.

In the untagged $\gamma\gamma$ event classes, where a 2D analysis using $m_{\gamma\gamma}$ and $\pi_T^{\gamma\gamma}$ is performed, it is necessary to define a signal model that is a function of these two observables, in the regions $100 < m_{\gamma\gamma} < 180$ GeV and $0.1 < \pi_T^{\gamma\gamma} < 2$. The correlations between the two variables are neglected, because the mass resolution of the Higgs boson has little dependence on its momentum. The PDF becomes a product of two one-dimensional PDFs, one for the mass and one for the second observable, $\mathcal{K}_s(\pi_T^{\gamma\gamma})$, empirically derived to be a sum of Gaussian and bifurcated Gaussian (a Gaussian PDF with different widths on left and right side of maximum value) functions. The π_T shape uncertainty contributes less than 1% to the expected exclusion limit.

3.1.5 Background modelling in dijet and lepton tag classes

For the dijet-tag event class, the background model is derived from data, by fitting the diphoton mass distributions over the range $100 < m_{\gamma\gamma} < 180$ GeV. The choice of the function used to fit the background and the choice of the range are made based on a study of the possible bias introduced by the two choices. The bias is studied for both the limit in the case of no signal and the measured signal strength in the case of a signal.

In case of the lepton-tag class, the requirement of an additional isolated lepton suppresses the contribution from QCD background processes. The remaining background is small, coming predominantly from electroweak processes. Its shape is derived from fitting the MC simulation for muon tags, and from fitting a combination of data and MC simulated events for electron tags. For the electron-tagged events, a control sample (CS) is derived from data by requiring one of the photons to be matched with a track. This CS represents the reducible background with enhanced statistics. The final shape for this channel is the sum of the fits to simulation and the CS, with the two components weighted by the cross sections of the main irreducible and reducible background processes. The sum is normalised to the data yield in the range 100–160 GeV.

Bias studies are performed using a number of generated pseudo-experiments with background only and signal plus background hypotheses. It is observed that using a second order polynomial fit to the range $100 < m_{\gamma\gamma} < 180$ GeV for the dijet-tagged events results in only a small bias in either excluding or finding a Higgs-boson signal in the mass range $110 < m_{\gamma\gamma} < 150$ GeV. In both cases the maximum bias is found to be at least five times smaller than the statistical uncertainties of the fit. For the lepton-tagged classes, it is found, from the same technique, that the small number of selected events allow the use of exponential functions for the fits without introducing any significant bias as compared to the statistical uncertainty.

The data distribution of $m_{\gamma\gamma}$ and the corresponding background models in the three tagged event classes are shown in figure 1. For the dijet-tagged class the statistical uncertainty bands computed from the fit are shown. For both the muon-tagged and electron-tagged classes, uncertainty bands are not shown. For these two classes the dominant statistical uncertainty on the background model is obtained from the number of events which are used to determine the normalisation of the fit.

3.1.6 Background modelling in the untagged classes

In the untagged $\gamma\gamma$ event classes, where a 2D analysis using $m_{\gamma\gamma}$ and $\pi_T^{\gamma\gamma}$ is performed, the background model is a distribution of these two observables. The nominal background PDF accounts for a linear correlation between the two observables and has the following form:

$$\mathcal{P}_b = \mathcal{M}_b(m_{\gamma\gamma}, \pi_T^{\gamma\gamma} | a_0, a_1) \times \mathcal{K}_b(\pi_T^{\gamma\gamma}) = m_{\gamma\gamma}^{a_0 + a_1 \pi_T^{\gamma\gamma}} \times \mathcal{K}_b(\pi_T^{\gamma\gamma}) \quad (3.1)$$

The empirical background PDF for the second observable, $\mathcal{K}_b(\pi_T^{\gamma\gamma})$ is defined as a sum of an exponential function (\mathcal{E}) of slope τ_B and a Gaussian function (\mathcal{G}) of width σ_G and mean fixed at zero:

$$\mathcal{K}_b(\pi_T^{\gamma\gamma} | \tau_B, f_d, \sigma_G) = f_d \mathcal{E}(\pi_T^{\gamma\gamma} | \tau_B) + (1 - f_d) \mathcal{G}(\pi_T^{\gamma\gamma} | 0, \sigma_G) \quad (3.2)$$

A power law function is chosen to describe the $m_{\gamma\gamma}$ distribution. The data in each of the four untagged event classes are fitted separately. Figures 2 and 3 show the data and the fit results projected on $m_{\gamma\gamma}$, and on $\pi_T^{\gamma\gamma}$, respectively, for each class.

Goodness-of-fit tests are performed measuring the bias of the model due to correlations between the two observables and due to choice of functional forms. Pseudo-experiments are

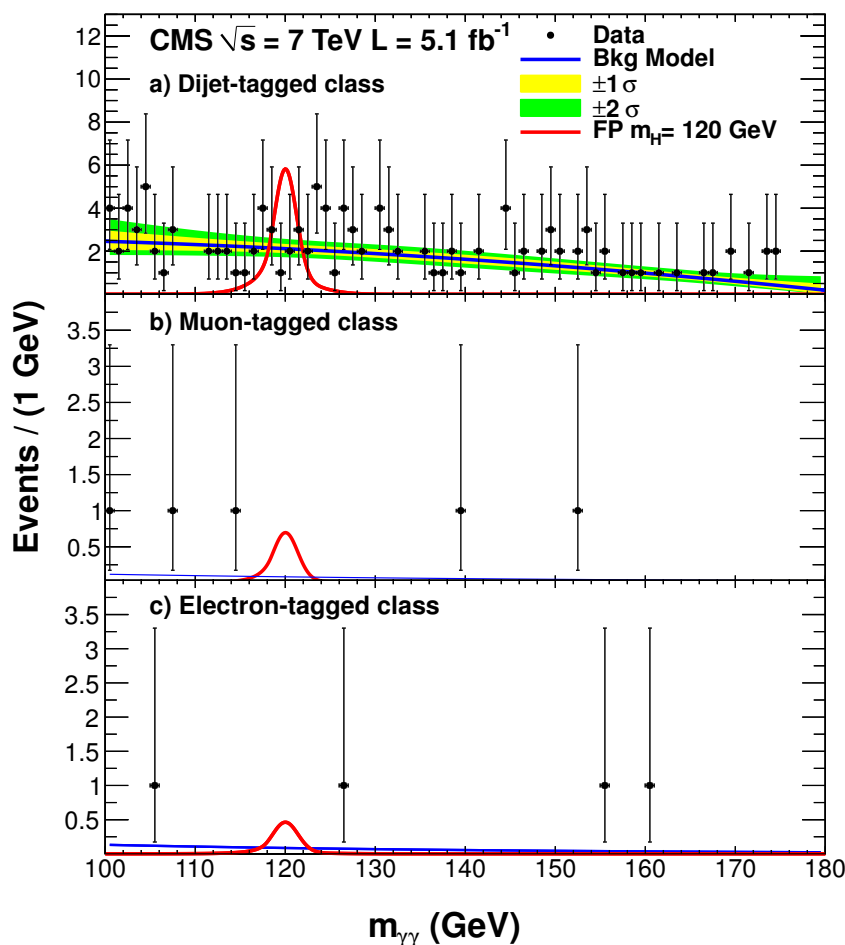


Figure 1. Data and the background model fits to the $m_{\gamma\gamma}$ distribution for the three diphoton event classes from tagging channels: for dijet-tag with a second order polynomial fit (top), muon-tag (middle) and electron-tag (bottom) with an exponential fit for the lepton-tag. For the two bottom plots the uncertainty bands are not shown, as explained in the text. Signal for an FP Higgs with a mass of 120 GeV is overlaid for reference.

performed, generated from alternative background models, and the signal plus background model is fitted for various test masses. The bias is taken as the mean of the pull distribution, which is defined as the difference between the fitted and generated signal strength divided by the statistical error from the fit in each event. If the pseudo-experiments are generated from a background model containing a linear correlation of the two variables, a maximum bias of 60% is observed if a linear correlation is not included in the fitting function. Tests have shown that with a linear plus quadratic correlation in the model a fit with only a linear correlation results in a bias of less than 13% in the entire fit range. This bias is regarded as negligible and thus it is concluded that a fit function with linear correlation is adequate. With a similar procedure, the nominal fit function is tested against alternative models of mass shape with functions including linear correlations. A maximum bias of about one quarter of the statistical error is measured, which is negligible.

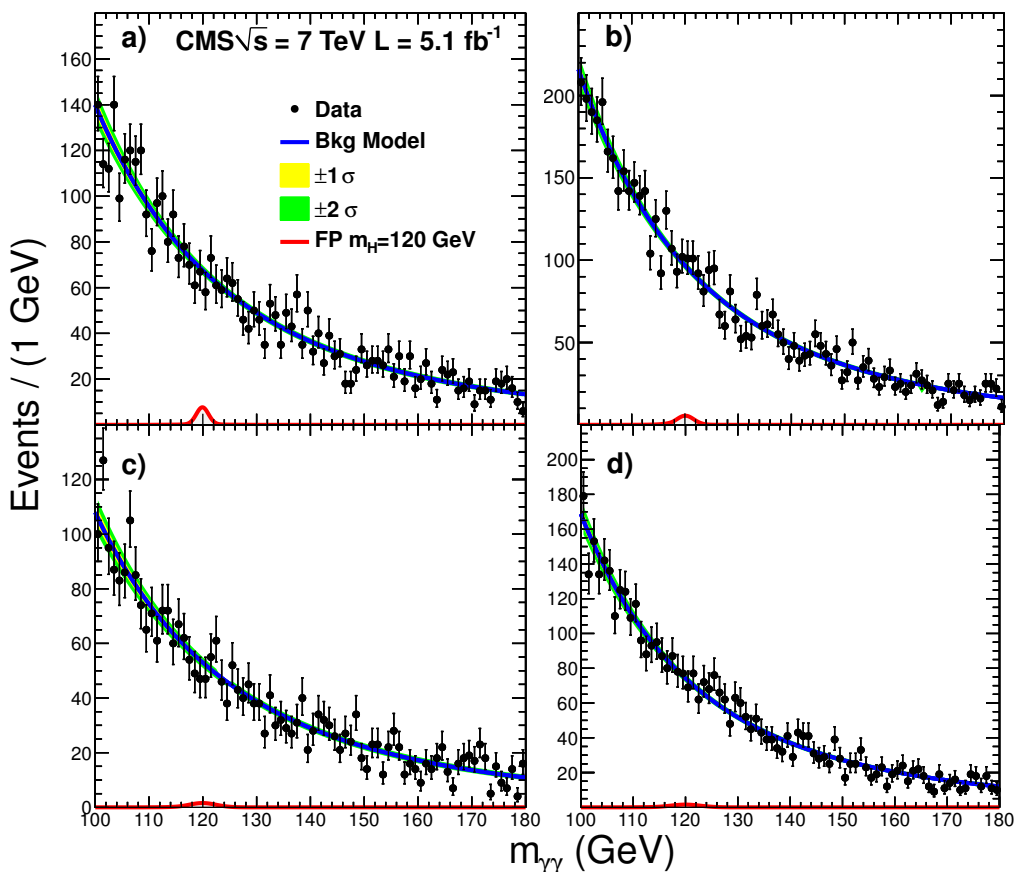


Figure 2. $m_{\gamma\gamma}$ distribution in data (points) in the four categories of the untagged $\gamma\gamma$ sub-channel (a)–(d) defined in section 3.1.3, together with background model fits of a power function including linear correlation to $\pi_T^{\gamma\gamma}$. An MC simulated FP Higgs boson signal ($m_H=120$ GeV) is overlaid for reference.

3.2 Diboson WW decay mode

3.2.1 Dijet tag event class

The $H \rightarrow WW^{(*)} \rightarrow 2\ell 2\nu$ analysis [18] selects events with two isolated leptons of opposite charge, large missing transverse energy, and two jets with VBF topology. One lepton is required to have $p_T > 20$ GeV, while the second is required to have $p_T > 10$ GeV. The fiducial region is $|\eta| < 2.4$ for muons and $|\eta| < 2.5$ for electrons. If the two leptons have the same flavour, the one with lower p_T is required to have a p_T of at least 15 GeV to suppress the Drell-Yan background. The missing transverse energy requirement is applied by means of a selection on the projected E_T^{miss} defined as the component of E_T^{miss} transverse to the nearest lepton if that lepton is within $\pi/2$ in azimuthal angle, or the full E_T^{miss} otherwise [37], which is required to be larger than about 40 GeV, the precise value depending on the number of vertices found in each event. Jets are required to have a $p_T > 30$ GeV and $|\eta| < 5$, and the two jets with the highest p_T are chosen as tag jets (j_1, j_2). The VBF selection requires $|\eta_{j_1} - \eta_{j_2}| > 3.5$ and $m_{j_1 j_2} > 450$ GeV. The distributions of $m_{j_1 j_2}$ and

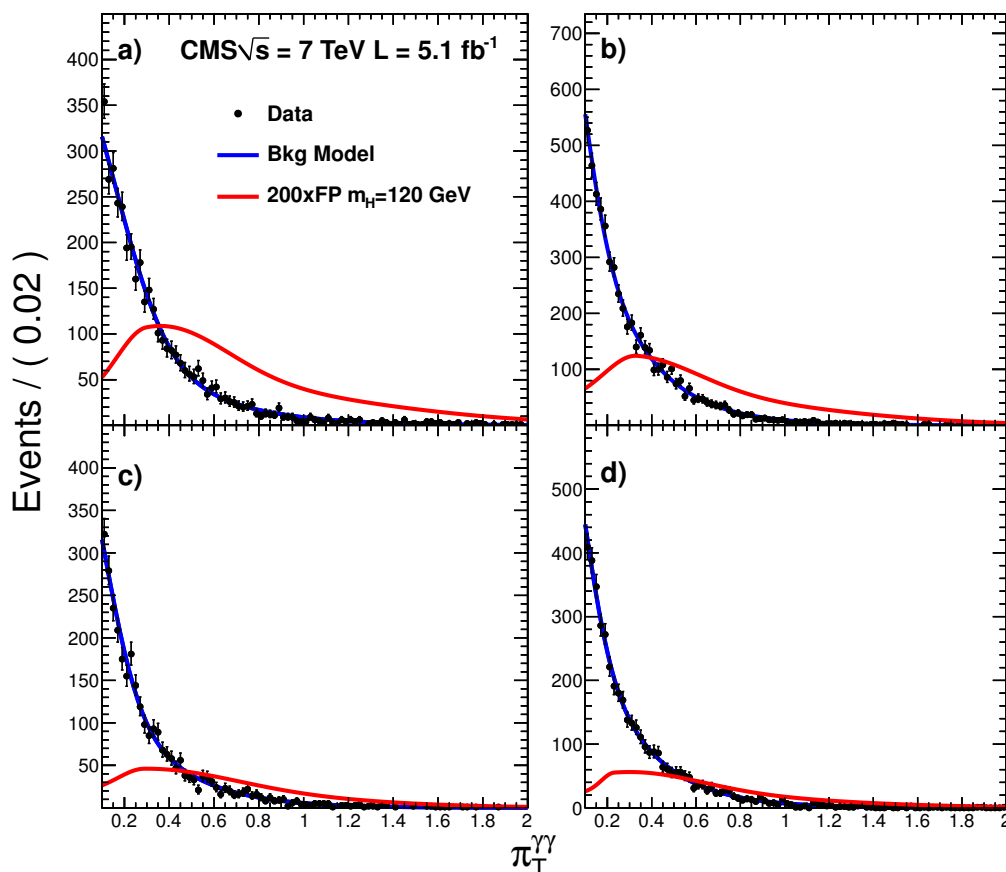


Figure 3. $\pi_T^{\gamma\gamma}$ distribution in data (points) in the four categories of the untagged $\gamma\gamma$ sub-channel (a)-(d) defined in section 3.1.3, together with background model fits of a sum of exponential and Gaussian functions centred at zero. A MC simulated FP Higgs boson signal ($m_H = 120$ GeV) is also shown, scaled by 200 and modelled with a sum of a Gaussian and a bifurcated Gaussian.

$\Delta\eta_{jj} = |\eta_{j_1} - \eta_{j_2}|$ are shown in figure 4 after the WW selection. Besides the cuts on the dijet system, it is required that the event has no other jets above 30 GeV found between the tag jets in pseudorapidity. These selections suppress the dominant background coming from top-quark production, which is also reduced by requiring a b-veto on the tag jets using jet impact parameters. The Drell-Yan background is suppressed by requirements on the dilepton system mass and momentum, as well as on the angle between the dilepton and the dijet system. Events with additional leptons above 10 GeV are rejected. After all requirements, between 10 and 20 data events remain in the signal regions which are defined according to the Higgs boson mass hypothesis [18]. These events are compatible with a background only hypothesis. The main backgrounds, namely $t\bar{t}$ and Z + jets, are estimated from the data: the $t\bar{t}$ is measured in the region where the central jet is b-tagged, while the Z + jets is measured under the Z peak. Also the contamination coming from W + jets and QCD is measured in data, in a phase space with relaxed lepton identification. The WW background is evaluated from simulation.

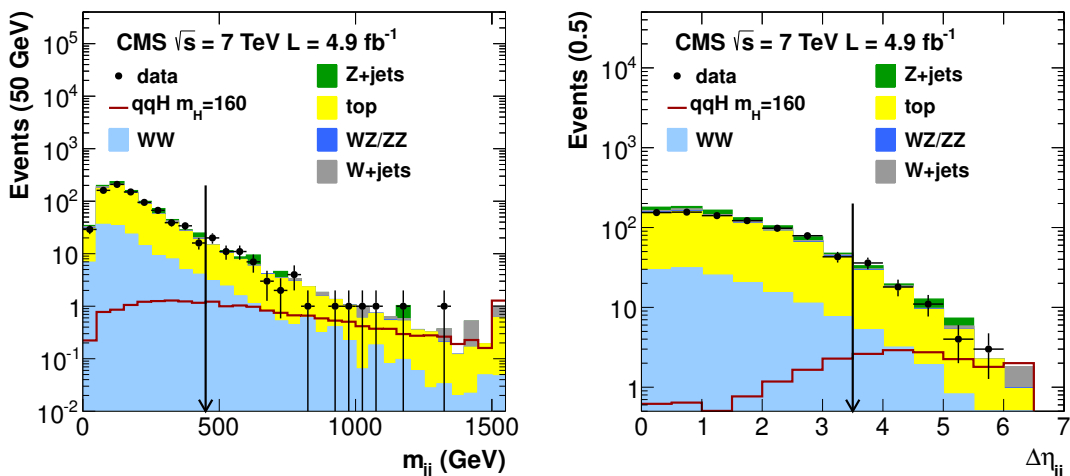


Figure 4. The distributions of $m_{j_1 j_2}$ (left) and $\Delta\eta_{jj} = |\eta_{j_1} - \eta_{j_2}|$ (right) after the WW selection. Contributions from backgrounds are shown together with data, and the expected signal from VBF production is shown for $m_H = 160$ GeV. The arrows show the minimum values in the selections applied for the WW dijet-tag analysis.

3.2.2 Zero and one-jet event classes

The results obtained by the inclusive analysis [18] in the zero and one-jet classes are also included in the limit extraction. The electron and muon selection is the same as for the dijet-tagged class. A p_T threshold of 30 GeV is placed on the jets, the number of which defines the classes. Events are split into same-flavour and different-flavour dilepton sub-channels, since the background from Drell-Yan production is much larger for the same-flavour dilepton events. The dominant background for these classes is from WW, together with Z + jets and top-quark production in the one-jet class, as well as contaminations from W + jets and QCD.

3.2.3 Lepton tag event class

The $WH \rightarrow WWW \rightarrow 3\ell 3\nu$ analysis selects events with three charged leptons, either electrons or muons, large E_T^{miss} , and low hadronic activity. The third lepton has to be isolated and have $p_T > 10$ GeV, and it is required that there be no jet with $p_T > 40$ GeV in the event. The dominant background comes from $WZ \rightarrow 3\ell\nu$ production, which is largely eliminated by requiring that the invariant mass of all same-flavour oppositely charged lepton pairs is not within ± 25 GeV of the nominal Z boson mass. In addition, the smallest dilepton mass $m_{\ell\ell}$ constructed from oppositely charged leptons is required to lie between 12 and 100 GeV, and the smallest distance, ΔR , between them is required to be less than 2. The background processes with jets misidentified as leptons, e.g. Z+jets and top, as well as the $WZ \rightarrow 3\ell\nu$ background are estimated from data. The small contribution from the $ZZ \rightarrow 4\ell$ process with one unreconstructed lepton is estimated using simulated samples. After all cuts, 7 data events remain in the signal region while 8.4 ± 0.9 events are expected from simulation.

3.2.4 Signal and background modelling

For the dijet and lepton tag WW classes, the hypothesis testing is based on the number of expected signal and background events only. Because of the impossibility to fully reconstruct the Higgs resonance and the small number of events expected in these classes, the limit extraction is based on counting experiments in both the VBF and WH sub-channels. The number of expected signal events is evaluated from simulation, while the background contamination in the signal regions is estimated with methods based on data whenever possible. For the zero and one jet classes, the limit extraction is based on the shape of a multi-variate discriminant, optimised to maximise the difference between the signal and the WW background. The discriminant is built on the kinematics of the dilepton pair and the missing energy. For the signal case, the model is obtained from the simulation; for most of the backgrounds, the templates are taken from the simulation and cross-checked in control samples in data. For the W + jets background the nominal shape is derived from a data control sample.

3.3 Diboson ZZ decay mode

In the $H \rightarrow ZZ^{(*)} \rightarrow 4\ell$ channel [19] a search is made for a four-lepton mass peak over a small continuum background. The $4e$, 4μ , $2e2\mu$ sub-channels are analysed separately since there are differences in the four-lepton mass resolutions and the background rates arising from jets misidentified as leptons. The dominant irreducible background in this channel is from non-resonant ZZ production (with both Z bosons decaying to either $2e$, or 2μ , or 2τ with the taus decaying leptonically) and is estimated from simulation. The smaller reducible backgrounds with jets misidentified as leptons, e.g. Z + jets, are estimated from data.

In the $H \rightarrow ZZ \rightarrow 2\ell 2\nu$ search [20], events are selected by the presence of a lepton pair (ee or $\mu\mu$), with invariant mass consistent with that of an on-shell Z boson, and a large E_T^{miss} . A transverse invariant mass m_T is defined from the dilepton momenta and E_T^{miss} , assuming that E_T^{miss} arises from a $Z \rightarrow \nu\nu$ decay. A broad excess of events is searched for in the m_T distribution. The non-resonant ZZ and WZ backgrounds are taken from simulation, while all other backgrounds are evaluated from control samples in data.

In the $H \rightarrow ZZ^{(*)} \rightarrow 2\ell 2q$ search [21], events are selected with two leptons (ee or $\mu\mu$) and two jets with zero, one, or two b-tags, thus defining a total of six exclusive final states. Requiring b-tagging improves the signal-to-background ratio. The two jets are required to form an invariant mass consistent with that of an on-shell Z boson. The aim is to search for a peak in the invariant mass distribution of the dilepton-dijet system, with the background rate and shape estimated using control regions in data.

In the $H \rightarrow ZZ \rightarrow 2\ell 2\tau$ search [22], one Z boson is required to be on-shell and to decay to a lepton pair (ee or $\mu\mu$). The other Z boson is required to decay through a $\tau\tau$ pair to one of the four final-state signatures $e\mu$, $e\tau_h$, $\mu\tau_h$, $\tau_h\tau_h$, where τ_h is a hadronically decaying τ . Thus, eight exclusive sub-channels are defined. A broad excess is searched for in the distribution of the dilepton-ditau mass, constructed from the visible products of the tau decays, neglecting the effect of the accompanying neutrinos. The dominant background

is non-resonant ZZ production whose rate is estimated from simulation. The main sub-leading backgrounds with jets misidentified as τ leptons stem from Z +jets (including ZW) and top-quark events. These backgrounds are estimated from data.

3.3.1 Signal and background modelling

The limit calculation for the ZZ classes is based on the shape of the invariant mass distribution of the decay products, and the likelihood is written in terms of the estimated probability distribution function for the signal and the background. For $H \rightarrow ZZ^{(*)} \rightarrow 4\ell$ and $H \rightarrow ZZ^{(*)} \rightarrow 2\ell 2q$, the signal shapes are described by means of analytical fits, based on the Crystal Ball function. For the $H \rightarrow ZZ \rightarrow 2\ell 2\tau$ class the likelihood is based on the binned distribution of the reconstructed visible mass. For the $H \rightarrow ZZ \rightarrow 2\ell 2\nu$ class the likelihood is based on the binned distribution of the transverse mass calculated using the visible decay products. The background shapes are extracted from data when possible, while for the irreducible ones, such as the electroweak ZZ or WZ production, the simulation is used.

4 Results

The statistical approach considered in evaluating the limit is the asymptotic CL_S [38] with the profile likelihood ratio as a test-statistic [39]. Given the narrowness of the Higgs mass peak in the $\gamma\gamma$ channel, which has a resolution approaching 1 GeV in the classes with the best resolution, the search is carried out with steps of 0.5 GeV in the signal hypothesis mass in the range between 110 and 150 GeV. All known sources of systematic uncertainties are included in the likelihood model which is used for the limit setting. Systematic errors which are correlated between event classes (theory, luminosity, photon and trigger efficiency, etc) are included as common nuisance parameters.

Following the prescription in [40], the QCD scale uncertainties on the FP Higgs boson production cross section are increased with respect to those of the SM Higgs boson, to 5%, to cover the effects of electroweak corrections which have not yet been calculated.

Figure 5 (left) shows the limit relative to the FP model expectation from the $\gamma\gamma$ sub-channels only, where the systematic uncertainties on the expected cross section and branching fraction are included in the limit setting procedure. The observed values are shown by a solid line. The contributions to the expected limit of each of the $\gamma\gamma$ sub-channels are also shown. The sensitivity of the search in this channel lies predominantly in the dijet tag sub-channel. The $\gamma\gamma$ combined expected exclusion limit at 95% CL covers the mass range between 110–136.5 GeV, while the data exclude ranges from 110–124.5 GeV and 127–137.5 GeV. Figure 5 (right) shows the local p -value for $\gamma\gamma$ channel and each sub-channel, calculated from the asymptotic approximation [39], at 0.5 GeV intervals in the mass range 110–150 GeV. The local p -value quantifies the probability for the background to produce a fluctuation at least as large as observed, and assumes that the relative signal strength between the event classes follows the MC signal model for the FP Higgs boson. The local p -value corresponding to the largest upwards fluctuation of the observed limit, at 125 GeV, has been computed to be 3.6×10^{-3} (2.7σ) in the asymptotic approximation. When taking

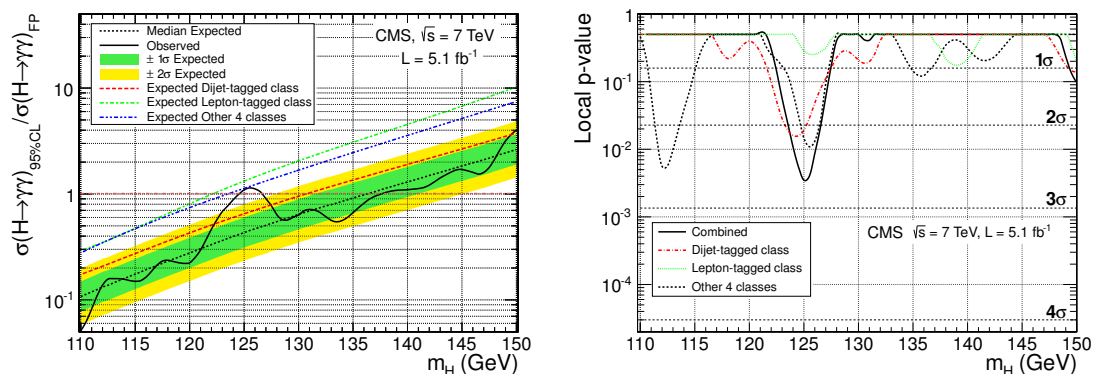


Figure 5. (Left) The 95% CL upper limit on the signal strength, σ/σ_{FP} , of an FP Higgs boson, as a function of the Higgs boson mass, for the $\gamma\gamma$ channel. The dashed line indicates the expected median of results for the background-only hypothesis, while the two bands indicate the ranges that are expected to contain 68% and 95% of all observed excursions from the median, respectively. The asymptotic CL_S method is used. Individual contributions to the expected limit for each of the channels are shown with dotted lines. (Right) The p -value of $\gamma\gamma$ channel. Contributions of individual sub-channels are also shown.

into consideration the look-elsewhere effect [41] in the search range 110–150 GeV, the global significance of this deviation is 1.2σ .

Figure 6 shows the 95% CL upper limit on the signal strength, σ/σ_{FP} , of an FP Higgs boson, as a function of the Higgs boson mass, for the WW channel. The contributions from the individual sub-channels are indicated. The limit from the dijet-tagged sub-channel complements the $\gamma\gamma$ search channels, excluding the FP hypothesis from 146 GeV to 196 GeV.

The 32 sub-channels of the three decay modes, $\gamma\gamma$, WW, and ZZ, described in section 3, are combined using the combination techniques described in ref. [39] to account for all statistical and systematic uncertainties and their correlations. The uncertainties consist of: theoretical uncertainties on the expected cross sections and acceptances for signal and background processes, experimental uncertainties in the modeling of the detector response (event reconstruction and selection efficiencies, energy scale and resolution), and statistical uncertainties associated with either ancillary measurements of backgrounds in control regions or selection efficiencies obtained using simulated events.

The limit on the signal strength, σ/σ_{FP} , of an FP Higgs boson, as a function of the Higgs boson mass, calculated using the asymptotic approximation, is shown in figure 7, together with the expected and observed 95% CL limits for individual fermiophobic Higgs boson decay modes as well as for their combination. Checks at a few test points around 125 GeV have shown the calculation to be consistent with values obtained by the full modified frequentist approach [42]. The fermiophobic Higgs boson is excluded at 95% CL in the mass range 110–194 GeV. At 99% CL, we exclude the fermiophobic Higgs boson in the range 110–188 GeV, with the exception of two gaps: 124.5–127 GeV and 147.5–155 GeV. The sensitivity of the search lies predominantly in the $\gamma\gamma$ channel below 140 GeV, and in the WW channel for the high mass search range.

The local p -value as a function of the Higgs boson mass is obtained using the asymptotic approximation for individual decay modes and for their combination, and is shown

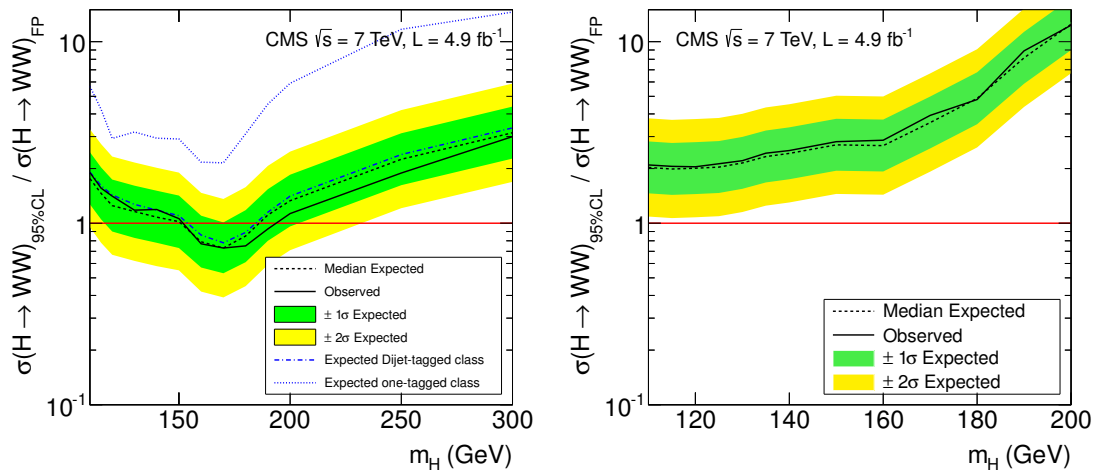


Figure 6. The 95% CL upper limit on the signal strength, σ/σ_{FP} , of an FP Higgs boson, as a function of the Higgs boson mass, for the WW channel. (Left) Limit for the WW final state excluding the WH trilepton sub-channel. The contributions to the expected limit from the dijet-tagged and the single jet event classes are also shown. (Right) Limit for the WH trilepton sub-channel. The dashed line indicates the expected median of results for the background-only hypothesis, while the two bands indicate the ranges that are expected to contain 68% and 95% of all observed excursions from the median, respectively. The asymptotic CL_S method is used.

in figure 8 (left). For a few points, the p -value calculation is checked with the frequentist approach [39] and is shown to agree within the statistical error. The local p -value corresponding to the largest upwards fluctuation of the observed limit, at 125 GeV, is computed to have a significance of 2.5σ . When taking into consideration the look-elsewhere effect [41] in the search range 110–300 GeV, the global significance of the deviation is 0.9σ . This deviation from the expected limit is too weak to be consistent with the fermiophobic Higgs boson signal, as can be seen in figure 8 (right), which shows the observed signal strength for an FP Higgs, as obtained from the fit of signal plus background on data. In this fit the constraint on signal strength being non-negative is not applied, so that a negative value indicates an observation below the expectation from the background-only hypothesis.

5 Summary

Combined results are reported from searches for a fermiophobic Higgs boson in proton-proton collisions at $\sqrt{s} = 7$ TeV in its decay modes into vector bosons: $\gamma\gamma$, WW, and ZZ, where the Higgs boson production is restricted to vector boson fusion and associated production with a vector boson. The Higgs boson mass range explored is 110–300 GeV. The data analyzed correspond to an integrated luminosity of 4.9–5.1 fb^{-1} . The fermiophobic Higgs boson is excluded at 95% CL in the mass range 110–194 GeV and at 99% CL in the mass ranges 110–124.5 GeV, 127–147.5 GeV, and 155–180 GeV.

Acknowledgments

We congratulate our colleagues in the CERN accelerator departments for the excellent performance of the LHC machine. We thank the technical and administrative staff at CERN

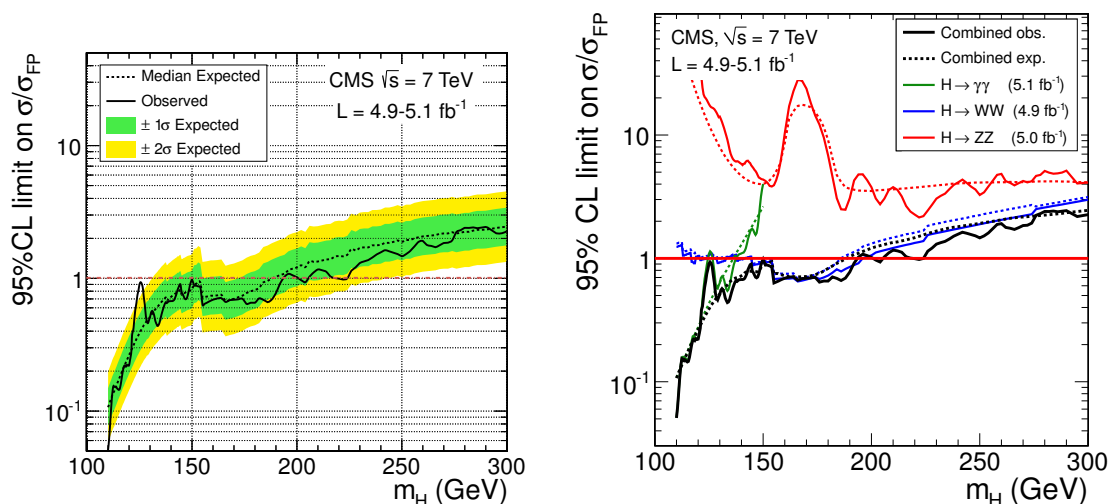


Figure 7. (Left) The observed and expected 95% CL upper limits on the signal strength, σ/σ_{FP} , for the fermiophobic Higgs boson hypothesis as a function of the Higgs boson mass. (Right): The observed and expected 95% CL upper limits on the signal strength as a function of the fermiophobic Higgs boson mass for the three explored Higgs boson decay modes and their combination.

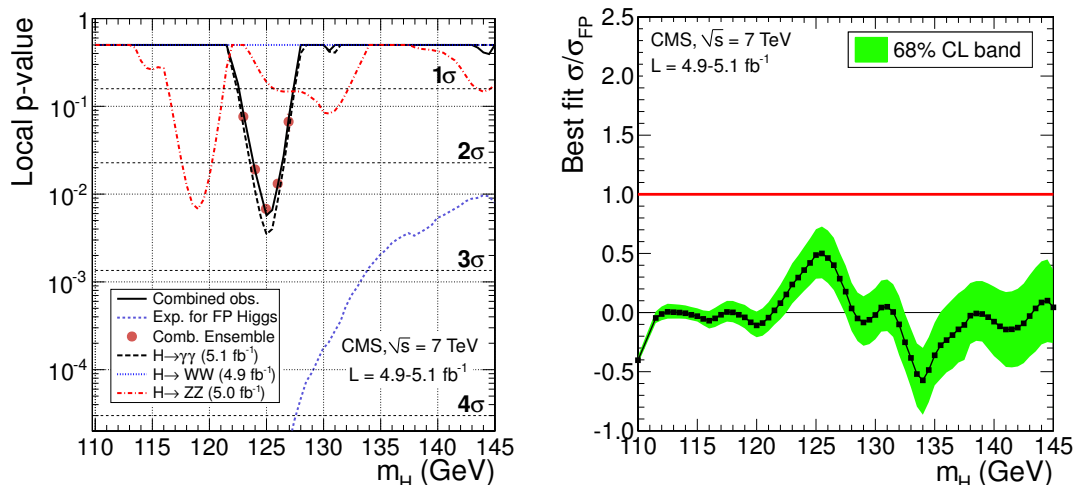


Figure 8. (Left) The observed and expected local p -values as a function of Higgs boson mass for the fermiophobic Higgs boson search. The local p -values for the three decay modes taken separately, and their combination are obtained with the asymptotic approximation; the combined local p -value is validated at a few m_H (dots) using the full frequentist approach by generating ensembles of background-only pseudo-datasets. The dashed line indicates the expected combined local p -value, should a fermiophobic Higgs boson with a mass m_H exist. (Right) The best-fit value of the signal strength, σ/σ_{FP} , for the combined sub-channels, as a function of the mass of a fermiophobic Higgs boson.

and other CMS institutes. This work was supported by the Austrian Federal Ministry of Science and Research; the Belgium Fonds de la Recherche Scientifique, and Fonds voor Wetenschappelijk Onderzoek; the Brazilian Funding Agencies (CNPq, CAPES, FAPERJ, and FAPESP); the Bulgarian Ministry of Education and Science; CERN; the Chinese

Academy of Sciences, Ministry of Science and Technology, and National Natural Science Foundation of China; the Colombian Funding Agency (COLCIENCIAS); the Croatian Ministry of Science, Education and Sport; the Research Promotion Foundation, Cyprus; the Ministry of Education and Research, Recurrent financing contract SF0690030s09 and European Regional Development Fund, Estonia; the Academy of Finland, Finnish Ministry of Education and Culture, and Helsinki Institute of Physics; the Institut National de Physique Nucléaire et de Physique des Particules / CNRS, and Commissariat à l'Énergie Atomique et aux Énergies Alternatives / CEA, France; the Bundesministerium für Bildung und Forschung, Deutsche Forschungsgemeinschaft, and Helmholtz-Gemeinschaft Deutscher Forschungszentren, Germany; the General Secretariat for Research and Technology, Greece; the National Scientific Research Foundation, and National Office for Research and Technology, Hungary; the Department of Atomic Energy and the Department of Science and Technology, India; the Institute for Studies in Theoretical Physics and Mathematics, Iran; the Science Foundation, Ireland; the Istituto Nazionale di Fisica Nucleare, Italy; the Korean Ministry of Education, Science and Technology and the World Class University program of NRF, Korea; the Lithuanian Academy of Sciences; the Mexican Funding Agencies (CINVESTAV, CONACYT, SEP, and UASLP-FAI); the Ministry of Science and Innovation, New Zealand; the Pakistan Atomic Energy Commission; the Ministry of Science and Higher Education and the National Science Centre, Poland; the Fundação para a Ciência e a Tecnologia, Portugal; JINR (Armenia, Belarus, Georgia, Ukraine, Uzbekistan); the Ministry of Education and Science of the Russian Federation, the Federal Agency of Atomic Energy of the Russian Federation, Russian Academy of Sciences, and the Russian Foundation for Basic Research; the Ministry of Science and Technological Development of Serbia; the Ministerio de Ciencia e Innovación, and Programa Consolider-Ingenio 2010, Spain; the Swiss Funding Agencies (ETH Board, ETH Zurich, PSI, SNF, UniZH, Canton Zurich, and SER); the National Science Council, Taipei; the Scientific and Technical Research Council of Turkey, and Turkish Atomic Energy Authority; the Science and Technology Facilities Council, UK; the US Department of Energy, and the US National Science Foundation. Individuals have received support from the Marie-Curie programme and the European Research Council (European Union); the Leventis Foundation; the A. P. Sloan Foundation; the Alexander von Humboldt Foundation; the Belgian Federal Science Policy Office; the Fonds pour la Formation à la Recherche dans l'Industrie et dans l'Agriculture (FRIA-Belgium); the Agentschap voor Innovatie door Wetenschap en Technologie (IWT-Belgium); the Council of Science and Industrial Research, India; and the HOMING PLUS programme of Foundation for Polish Science, cofinanced from European Union, Regional Development Fund.

Open Access. This article is distributed under the terms of the Creative Commons Attribution License which permits any use, distribution and reproduction in any medium, provided the original author(s) and source are credited.

References

- [1] F. Englert and R. Brout, *Broken symmetry and the mass of gauge vector mesons*, *Phys. Rev. Lett.* **13** (1964) 321 [[INSPIRE](#)].

- [2] P.W. Higgs, *Broken symmetries, massless particles and gauge fields*, *Phys. Lett.* **12** (1964) 132 [INSPIRE].
- [3] A. Akeroyd, *Higgs triplets at LEP-2*, *Phys. Lett.* **B 353** (1995) 519 [INSPIRE].
- [4] A. Akeroyd, *Fermiophobic Higgs bosons at the Tevatron*, *Phys. Lett.* **B 368** (1996) 89 [hep-ph/9511347] [INSPIRE].
- [5] H. Haber, G.L. Kane and T. Sterling, *The Fermion mass scale and possible effects of Higgs bosons on experimental observables*, *Nucl. Phys.* **B 161** (1979) 493 [INSPIRE].
- [6] A.G. Akeroyd, *Fermiophobic and other nonminimal neutral Higgs bosons at the LHC*, *J. Phys. G* **G 24** (1998) 1983 [hep-ph/9803324] [INSPIRE].
- [7] E. Gabrielli and B. Mele, *Testing effective Yukawa couplings in Higgs searches at the Tevatron and LHC*, *Phys. Rev.* **D 82** (2010) 113014 [Erratum *ibid.* **D 83** (2011) 079901] [arXiv:1005.2498] [INSPIRE].
- [8] LEP HIGGS WORKING GROUP, ALEPH, DELPHI, L3, OPAL collaboration, *Searches for Higgs bosons decaying into photons: Preliminary combined results using LEP data collected at energies up to 209 GeV*, *hep-ex/0107035* [INSPIRE].
- [9] ALEPH collaboration, *Search for $\gamma\gamma$ decays of a Higgs boson produced in association with a fermion pair in e^+e^- collisions at LEP*, *Phys. Lett.* **B 487** (2000) 241 [hep-ex/0008004] [INSPIRE].
- [10] DELPHI collaboration, *Search for a fermiophobic Higgs at LEP-2*, *Phys. Lett.* **B 507** (2001) 89 [hep-ex/0104025] [INSPIRE].
- [11] L3 collaboration, *Search for a Higgs boson decaying into two photons in e^+e^- interactions at $\sqrt{s} = 189$ GeV*, *Phys. Lett.* **B 489** (2000) 115 [hep-ex/0008025] [INSPIRE].
- [12] OPAL collaboration, *Search for Higgs bosons and other massive states decaying into two photons in e^+e^- collisions at 189 GeV*, *Phys. Lett.* **B 464** (1999) 311 [hep-ex/9907060] [INSPIRE].
- [13] CDF, D0, TEVATRON NEW HIGGS WORKING GROUP collaboration, *Combined CDF and D0 upper limits on fermiophobic Higgs boson production with up to 8.2 fb^{-1} of $p\bar{p}$ data*, *arXiv:1109.0576* [INSPIRE].
- [14] T. Aaltonen et al., *Search for a fermiophobic Higgs boson decaying into diphotons in pp collisions at $\sqrt{s} = 1.96$ TeV*, *Phys. Rev. Lett.* **103** (2009) 061803 [arXiv:0905.0413] [INSPIRE].
- [15] V.M. Abazov et al., *Search for resonant diphoton production with the D0 detector*, *Phys. Rev. Lett.* **102** (2009) 231801 [arXiv:0901.1887] [INSPIRE].
- [16] ATLAS collaboration, A. Collaboration et al., *Search for a fermiophobic Higgs boson in the diphoton decay channel with the ATLAS detector*, *arXiv:1205.0701* [INSPIRE].
- [17] CMS collaboration, S. Chatrchyan et al., *Search for the standard model Higgs boson decaying into two photons in pp collisions at $\sqrt{s} = 7$ TeV*, *Phys. Lett.* **B 710** (2012) 403 [arXiv:1202.1487] [INSPIRE].
- [18] CMS collaboration, S. Chatrchyan et al., *Search for the standard model Higgs boson decaying to a W pair in the fully leptonic final state in pp collisions at $\sqrt{s} = 7$ TeV*, *Phys. Lett.* **B 710** (2012) 91 [arXiv:1202.1489] [INSPIRE].

- [19] CMS collaboration, S. Chatrchyan et al., *Search for the standard model Higgs boson in the decay channel $H \rightarrow ZZ \rightarrow 4$ leptons in pp collisions at $\sqrt{s} = 7$ TeV*, *Phys. Rev. Lett.* **108** (2012) 111804 [[arXiv:1202.1997](#)] [[INSPIRE](#)].
- [20] CMS collaboration, S. Chatrchyan et al., *Search for the standard model Higgs boson in the $H \rightarrow ZZ \rightarrow 2l2\nu$ channel in pp collisions at $\sqrt{s} = 7$ TeV*, *JHEP* **03** (2012) 040 [[arXiv:1202.3478](#)] [[INSPIRE](#)].
- [21] CMS collaboration, S. Chatrchyan et al., *Search for a Higgs boson in the decay channel $H \rightarrow ZZ^{(*)} \rightarrow q\bar{q}l^{-}l^{+}$ in pp collisions at $\sqrt{s} = 7$ TeV*, *JHEP* **04** (2012) 036 [[arXiv:1202.1416](#)] [[INSPIRE](#)].
- [22] CMS collaboration, S. Chatrchyan et al., *Search for the standard model Higgs boson in the $H \rightarrow ZZ \rightarrow ll\tau\tau$ decay channel in pp collisions at $\sqrt{s} = 7$ TeV*, *JHEP* **03** (2012) 081 [[arXiv:1202.3617](#)] [[INSPIRE](#)].
- [23] CMS collaboration, S. Chatrchyan et al., *The CMS experiment at the CERN LHC*, 2008 *JINST* **3** S08004 [[INSPIRE](#)].
- [24] LHC HIGGS CROSS SECTION WORKING GROUP collaboration, S. Dittmaier et al., *Handbook of LHC Higgs cross sections: 1. Inclusive observables*, [arXiv:1101.0593](#) [[INSPIRE](#)].
- [25] K. Arnold et al., *VBFNLO: a parton level Monte Carlo for processes with electroweak bosons*, *Comput. Phys. Commun.* **180** (2009) 1661 [[arXiv:0811.4559](#)] [[INSPIRE](#)].
- [26] P. Bolzoni, F. Maltoni, S.-O. Moch and M. Zaro, *Higgs production via vector-boson fusion at NNLO in QCD*, *Phys. Rev. Lett.* **105** (2010) 011801 [[arXiv:1003.4451](#)] [[INSPIRE](#)].
- [27] O. Brein, A. Djouadi and R. Harlander, *NNLO QCD corrections to the Higgs-strahlung processes at hadron colliders*, *Phys. Lett. B* **579** (2004) 149 [[hep-ph/0307206](#)] [[INSPIRE](#)].
- [28] M. Ciccolini, S. Dittmaier and M. Krämer, *Electroweak radiative corrections to associated WH and ZH production at hadron colliders*, *Phys. Rev. D* **68** (2003) 073003 [[hep-ph/0306234](#)] [[INSPIRE](#)].
- [29] A. Djouadi, J. Kalinowski and M. Spira, *HDECAY: a program for Higgs boson decays in the standard model and its supersymmetric extension*, *Comput. Phys. Commun.* **108** (1998) 56 [[hep-ph/9704448](#)] [[INSPIRE](#)].
- [30] J. Butterworth et al., *The tools and Monte Carlo working group summary report*, [arXiv:1003.1643](#) [[INSPIRE](#)].
- [31] T. Sjöstrand, S. Mrenna and P.Z. Skands, *PYTHIA 6.4 physics and manual*, *JHEP* **05** (2006) 026 [[hep-ph/0603175](#)] [[INSPIRE](#)].
- [32] GEANT4 collaboration, S. Agostinelli et al., *GEANT4: a simulation toolkit*, *Nucl. Instrum. Meth. A* **506** (2003) 250 [[INSPIRE](#)].
- [33] M. Cacciari, G.P. Salam and G. Soyez, *The anti- k_t jet clustering algorithm*, *JHEP* **04** (2008) 063 [[arXiv:0802.1189](#)] [[INSPIRE](#)].
- [34] D.L. Rainwater, R. Szalapski and D. Zeppenfeld, *Probing color singlet exchange in $Z + two$ jet events at the CERN LHC*, *Phys. Rev. D* **54** (1996) 6680 [[hep-ph/9605444](#)] [[INSPIRE](#)].
- [35] A. Ballestrero, G. Bevilacqua and E. Maina, *A complete parton level analysis of boson-boson scattering and electroweak symmetry breaking in $lv + four$ jets production at the LHC*, *JHEP* **05** (2009) 015 [[arXiv:0812.5084](#)] [[INSPIRE](#)].

- [36] J.E. Gaiser, *Charmonium spectroscopy from radiative decays of the J/Ψ and Ψ'* , Ph.D. Thesis, Stanford University, U.S.A. (1982).
- [37] CDF collaboration, T. Aaltonen et al., *Measurement of the W^+W^- production cross section and search for anomalous $WW\gamma$ and WWZ couplings in $p\bar{p}$ collisions at $\sqrt{s} = 1.96$ TeV*, *Phys. Rev. Lett.* **104** (2010) 201801 [[arXiv:0912.4500](#)] [[INSPIRE](#)].
- [38] G. Cowan, K. Cranmer, E. Gross and O. Vitells, *Asymptotic formulae for likelihood-based tests of new physics*, *Eur. Phys. J. C* **71** (2011) 1554 [[arXiv:1007.1727](#)] [[INSPIRE](#)].
- [39] ATLAS and CMS collaboration, LHC HIGGS COMBINATION GROUP, *Procedure for the LHC Higgs boson search combination in summer 2011*, [CMS-NOTE-2011-005](#) (2011).
- [40] LHC HIGGS CROSS SECTION WORKING GROUP, *Handbook of LHC Higgs cross sections: 2. Differential distributions*, [CERN-2012-002](#) (2012).
- [41] E. Gross and O. Vitells, *Trial factors or the look elsewhere effect in high energy physics*, *Eur. Phys. J. C* **70** (2010) 525 [[arXiv:1005.1891](#)] [[INSPIRE](#)].
- [42] A.L. Read, *Presentation of search results: The $CL(s)$ technique*, *J. Phys. G* **28** (2002) 2693 [[INSPIRE](#)].

The CMS collaboration

Yerevan Physics Institute, Yerevan, Armenia

S. Chatrchyan, V. Khachatryan, A.M. Sirunyan, A. Tumasyan

Institut für Hochenergiephysik der OeAW, Wien, Austria

W. Adam, E. Aguilo, T. Bergauer, M. Dragicevic, J. Erö, C. Fabjan¹, M. Friedl, R. Frühwirth¹, V.M. Ghete, J. Hammer, N. Hörmann, J. Hrubec, M. Jeitler¹, W. Kiesenhofer, V. Knünz, M. Krammer¹, D. Liko, I. Mikulec, M. Pernicka[†], B. Rahbaran, C. Rohringer, H. Rohringer, R. Schöfbeck, J. Strauss, A. Taurok, P. Wagner, W. Waltenberger, G. Walzel, E. Widl, C.-E. Wulz¹

National Centre for Particle and High Energy Physics, Minsk, Belarus

V. Mossolov, N. Shumeiko, J. Suarez Gonzalez

Universiteit Antwerpen, Antwerpen, Belgium

S. Bansal, T. Cornelis, E.A. De Wolf, X. Janssen, S. Luyckx, L. Mucibello, S. Ochesanu, B. Roland, R. Rougny, M. Selvaggi, Z. Staykova, H. Van Haevermaet, P. Van Mechelen, N. Van Remortel, A. Van Spilbeeck

Vrije Universiteit Brussel, Brussel, Belgium

F. Blekman, S. Blyweert, J. D'Hondt, R. Gonzalez Suarez, A. Kalogeropoulos, M. Maes, A. Olbrechts, W. Van Doninck, P. Van Mulders, G.P. Van Onsem, I. Villella

Université Libre de Bruxelles, Bruxelles, Belgium

B. Clerbaux, G. De Lentdecker, V. Dero, A.P.R. Gay, T. Hreus, A. Léonard, P.E. Marage, T. Reis, L. Thomas, C. Vander Velde, P. Vanlaer, J. Wang

Ghent University, Ghent, Belgium

V. Adler, K. Beernaert, A. Cimmino, S. Costantini, G. Garcia, M. Grunewald, B. Klein, J. Lellouch, A. Marinov, J. McCartin, A.A. Ocampo Rios, D. Ryckbosch, N. Strobbe, F. Thyssen, M. Tytgat, P. Verwilligen, S. Walsh, E. Yazgan, N. Zaganidis

Université Catholique de Louvain, Louvain-la-Neuve, Belgium

S. Basesmez, G. Bruno, R. Castello, L. Ceard, C. Delaere, T. du Pree, D. Favart, L. Forthomme, A. Giammanco², J. Hollar, V. Lemaitre, J. Liao, O. Militaru, C. Nuttens, D. Pagano, A. Pin, K. Piotrkowski, N. Schul, J.M. Vizan Garcia

Université de Mons, Mons, Belgium

N. Bely, T. Caebergs, E. Daubie, G.H. Hammad

Centro Brasileiro de Pesquisas Fisicas, Rio de Janeiro, Brazil

G.A. Alves, M. Correa Martins Junior, D. De Jesus Damiao, T. Martins, M.E. Pol, M.H.G. Souza

Universidade do Estado do Rio de Janeiro, Rio de Janeiro, Brazil

W.L. Aldá Júnior, W. Carvalho, A. Custódio, E.M. Da Costa, C. De Oliveira Martins, S. Fonseca De Souza, D. Matos Figueiredo, L. Mundim, H. Nogima, V. Oguri, W.L. Prado Da Silva, A. Santoro, L. Soares Jorge, A. Sznajder

Instituto de Fisica Teorica, Universidade Estadual Paulista, Sao Paulo, Brazil

C.A. Bernardes³, F.A. Dias⁴, T.R. Fernandez Perez Tomei, E. M. Gregores³, C. Lagana, F. Marinho, P.G. Mercadante³, S.F. Novaes, Sandra S. Padula

Institute for Nuclear Research and Nuclear Energy, Sofia, Bulgaria

V. Genchev⁵, P. Iaydjiev⁵, S. Piperov, M. Rodozov, S. Stoykova, G. Sultanov, V. Tcholakov, R. Trayanov, M. Vutova

University of Sofia, Sofia, Bulgaria

A. Dimitrov, R. Hadjiiska, V. Kozhuharov, L. Litov, B. Pavlov, P. Petkov

Institute of High Energy Physics, Beijing, China

J.G. Bian, G.M. Chen, H.S. Chen, C.H. Jiang, D. Liang, S. Liang, X. Meng, J. Tao, J. Wang, X. Wang, Z. Wang, H. Xiao, M. Xu, J. Zang, Z. Zhang

State Key Lab. of Nucl. Phys. and Tech., Peking University, Beijing, China

C. Asawatangtrakuldee, Y. Ban, S. Guo, Y. Guo, W. Li, S. Liu, Y. Mao, S.J. Qian, H. Teng, D. Wang, L. Zhang, B. Zhu, W. Zou

Universidad de Los Andes, Bogota, Colombia

C. Avila, J.P. Gomez, B. Gomez Moreno, A.F. Osorio Oliveros, J.C. Sanabria

Technical University of Split, Split, Croatia

N. Godinovic, D. Lelas, R. Plestina⁶, D. Polic, I. Puljak⁵

University of Split, Split, Croatia

Z. Antunovic, M. Kovac

Institute Rudjer Boskovic, Zagreb, Croatia

V. Brigljevic, S. Duric, K. Kadija, J. Luetic, S. Morovic

University of Cyprus, Nicosia, Cyprus

A. Attikis, M. Galanti, G. Mavromanolakis, J. Mousa, C. Nicolaou, F. Ptochos, P.A. Razis

Charles University, Prague, Czech Republic

M. Finger, M. Finger Jr.

Academy of Scientific Research and Technology of the Arab Republic of Egypt, Egyptian Network of High Energy Physics, Cairo, Egypt

Y. Assran⁷, S. Elgammal⁸, A. Ellithi Kamel⁹, S. Khalil⁸, M.A. Mahmoud¹⁰, A. Radi^{11,12}

National Institute of Chemical Physics and Biophysics, Tallinn, Estonia

M. Kadastik, M. Müntel, M. Raidal, L. Rebane, A. Tiko

Department of Physics, University of Helsinki, Helsinki, Finland

P. Eerola, G. Fedi, M. Voutilainen

Helsinki Institute of Physics, Helsinki, Finland

J. Härkönen, A. Heikkinen, V. Karimäki, R. Kinnunen, M.J. Kortelainen, T. Lampén, K. Lassila-Perini, S. Lehti, T. Lindén, P. Luukka, T. Mäenpää, T. Peltola, E. Tuominen, J. Tuominiemi, E. Tuovinen, D. Ungaro, L. Wendland

Lappeenranta University of Technology, Lappeenranta, Finland

K. Banzuzi, A. Karjalainen, A. Korpela, T. Tuuva

DSM/IRFU, CEA/Saclay, Gif-sur-Yvette, France

M. Besancon, S. Choudhury, M. Dejardin, D. Denegri, B. Fabbro, J.L. Faure, F. Ferri, S. Ganjour, A. Givernaud, P. Gras, G. Hamel de Monchenault, P. Jarry, E. Locci, J. Malcles, L. Millischer, A. Nayak, J. Rander, A. Rosowsky, I. Shreyber, M. Titov

Laboratoire Leprince-Ringuet, Ecole Polytechnique, IN2P3-CNRS, Palaiseau, FranceS. Baffioni, F. Beaudette, L. Benhabib, L. Bianchini, M. Bluj¹³, C. Broutin, P. Busson, C. Charlot, N. Daci, T. Dahms, L. Dobrzynski, R. Granier de Cassagnac, M. Haguenaer, P. Miné, C. Mironov, M. Nguyen, C. Ochando, P. Paganini, D. Sabes, R. Salerno, Y. Sirois, C. Veelken, A. Zabi**Institut Pluridisciplinaire Hubert Curien, Université de Strasbourg, Université de Haute Alsace Mulhouse, CNRS/IN2P3, Strasbourg, France**J.-L. Agram¹⁴, J. Andrea, D. Bloch, D. Bodin, J.-M. Brom, M. Cardaci, E.C. Chabert, C. Collard, E. Conte¹⁴, F. Drouhin¹⁴, C. Ferro, J.-C. Fontaine¹⁴, D. Gelé, U. Goerlach, P. Juillot, A.-C. Le Bihan, P. Van Hove**Centre de Calcul de l'Institut National de Physique Nucleaire et de Physique des Particules (IN2P3), Villeurbanne, France**

F. Fassi, D. Mercier

Université de Lyon, Université Claude Bernard Lyon 1, CNRS-IN2P3, Institut de Physique Nucléaire de Lyon, Villeurbanne, FranceS. Beauceron, N. Beaupere, O. Bondu, G. Boudoul, J. Chasserat, R. Chierici⁵, D. Contardo, P. Depasse, H. El Mamouni, J. Fay, S. Gascon, M. Gouzevitch, B. Ille, T. Kurca, M. Lethuillier, L. Mirabito, S. Perries, V. Sordini, S. Tosi, Y. Tschudi, P. Verdier, S. Viret**Institute of High Energy Physics and Informatization, Tbilisi State University, Tbilisi, Georgia**Z. Tsamalaidze¹⁵**RWTH Aachen University, I. Physikalisches Institut, Aachen, Germany**G. Anagnostou, S. Beranek, M. Edelhoff, L. Feld, N. Heracleous, O. Hindrichs, R. Jussen, K. Klein, J. Merz, A. Ostapchuk, A. Perieanu, F. Raupach, J. Sammet, S. Schael, D. Sprenger, H. Weber, B. Wittmer, V. Zhukov¹⁶**RWTH Aachen University, III. Physikalisches Institut A, Aachen, Germany**

M. Ata, J. Caudron, E. Dietz-Laursonn, D. Duchardt, M. Erdmann, R. Fischer, A. Güth, T. Hebbeker, C. Heidemann, K. Hoepfner, D. Klingebiel, P. Kreuzer, J. Lingemann, C. Magass, M. Merschmeyer, A. Meyer, M. Olschewski, P. Papacz, H. Pieta, H. Reithler, S.A. Schmitz, L. Sonnenschein, J. Steggemann, D. Teyssier, M. Weber

RWTH Aachen University, III. Physikalisches Institut B, Aachen, Germany

M. Bontenackels, V. Cherepanov, G. Flügge, H. Geenen, M. Geisler, W. Haj Ahmad, F. Hoehle, B. Kargoll, T. Kress, Y. Kuessel, A. Nowack, L. Perchalla, O. Pooth, J. Renefeld, P. Sauerland, A. Stahl

Deutsches Elektronen-Synchrotron, Hamburg, Germany

M. Aldaya Martin, J. Behr, W. Behrenhoff, U. Behrens, M. Bergholz¹⁷, A. Bethani, K. Borras, A. Burgmeier, A. Cakir, L. Calligaris, A. Campbell, E. Castro, F. Costanza, D. Dammann, C. Diez Pardos, G. Eckerlin, D. Eckstein, G. Flucke, A. Geiser, I. Glushkov, P. Gunnellini, S. Habib, J. Hauk, G. Hellwig, H. Jung, M. Kasemann, P. Katsas, C. Kleinwort, H. Kluge, A. Knutsson, M. Krämer, D. Krücker, E. Kuznetsova, W. Lange, W. Lohmann¹⁷, B. Lutz, R. Mankel, I. Marfin, M. Marienfeld, I.-A. Melzer-Pellmann, A.B. Meyer, J. Mnich, A. Mussgiller, S. Naumann-Emme, J. Olzem, H. Perrey, A. Petrukhin, D. Pitzl, A. Raspereza, P.M. Ribeiro Cipriano, C. Riedl, E. Ron, M. Rosin, J. Salfeld-Nebgen, R. Schmidt¹⁷, T. Schoerner-Sadenius, N. Sen, A. Spiridonov, M. Stein, R. Walsh, C. Wissing

University of Hamburg, Hamburg, Germany

C. Autermann, V. Blobel, J. Draeger, H. Enderle, J. Erfle, U. Gebbert, M. Görner, T. Hermanns, R.S. Höing, K. Kaschube, G. Kaussen, H. Kirschenmann, R. Klanner, J. Lange, B. Mura, F. Nowak, T. Peiffer, N. Pietsch, D. Rathjens, C. Sander, H. Schettler, P. Schlexer, E. Schlieckau, A. Schmidt, M. Schröder, T. Schum, M. Seidel, V. Sola, H. Stadie, G. Steinbrück, J. Thomsen, L. Vanelderen

Institut für Experimentelle Kernphysik, Karlsruhe, Germany

C. Barth, J. Berger, C. Böser, T. Chwalek, W. De Boer, A. Descroix, A. Dierlamm, M. Feindt, M. Guthoff⁵, C. Hackstein, F. Hartmann, T. Hauth⁵, M. Heinrich, H. Held, K.H. Hoffmann, S. Honc, I. Katkov¹⁶, J.R. Komaragiri, P. Lobelle Pardo, D. Martschei, S. Mueller, Th. Müller, M. Niegel, A. Nürnberg, O. Oberst, A. Oehler, J. Ott, G. Quast, K. Rabbertz, F. Ratnikov, N. Ratnikova, S. Röcker, A. Scheurer, F.-P. Schilling, G. Schott, H.J. Simonis, F.M. Stober, D. Troendle, R. Ulrich, J. Wagner-Kuhr, S. Wayand, T. Weiler, M. Zeise

Institute of Nuclear Physics "Demokritos", Aghia Paraskevi, Greece

G. Daskalakis, T. Geralis, S. Kesisoglou, A. Kyriakis, D. Loukas, I. Manolakos, A. Markou, C. Markou, C. Mavrommatis, E. Ntomari

University of Athens, Athens, Greece

L. Gouskos, T.J. Mertzimekis, A. Panagiotou, N. Saoulidou

University of Ioánnina, Ioánnina, Greece

I. Evangelou, C. Foudas⁵, P. Kokkas, N. Manthos, I. Papadopoulos, V. Patras

KFKI Research Institute for Particle and Nuclear Physics, Budapest, Hungary

G. Bencze, C. Hajdu⁵, P. Hidas, D. Horvath¹⁸, F. Sikler, V. Veszpremi, G. Vesztergombi¹⁹

Institute of Nuclear Research ATOMKI, Debrecen, Hungary

N. Beni, S. Czellar, J. Molnar, J. Palinkas, Z. Szillasi

University of Debrecen, Debrecen, Hungary

J. Karancsi, P. Raics, Z.L. Trocsanyi, B. Ujvari

Panjab University, Chandigarh, India

S.B. Beri, V. Bhatnagar, N. Dhingra, R. Gupta, M. Jindal, M. Kaur, M.Z. Mehta, N. Nishu, L.K. Saini, A. Sharma, J. Singh

University of Delhi, Delhi, India

Ashok Kumar, Arun Kumar, S. Ahuja, A. Bhardwaj, B.C. Choudhary, S. Malhotra, M. Naimuddin, K. Ranjan, V. Sharma, R.K. Shivpuri

Saha Institute of Nuclear Physics, Kolkata, India

S. Banerjee, S. Bhattacharya, S. Dutta, B. Gomber, Sa. Jain, Sh. Jain, R. Khurana, S. Sarkar, M. Sharan

Bhabha Atomic Research Centre, Mumbai, India

A. Abdulsalam, R.K. Choudhury, D. Dutta, S. Kailas, V. Kumar, P. Mehta, A.K. Mohanty⁵, L.M. Pant, P. Shukla

Tata Institute of Fundamental Research - EHEP, Mumbai, India

T. Aziz, S. Ganguly, M. Guchait²⁰, M. Maity²¹, G. Majumder, K. Mazumdar, G.B. Mohanty, B. Parida, K. Sudhakar, N. Wickramage

Tata Institute of Fundamental Research - HECR, Mumbai, India

S. Banerjee, S. Dugad

Institute for Research in Fundamental Sciences (IPM), Tehran, Iran

H. Arfaei, H. Bakhshiansohi²², S.M. Etesami²³, A. Fahim²², M. Hashemi, H. Hesari, A. Jafari²², M. Khakzad, M. Mohammadi Najafabadi, S. Paktinat Mehdiabadi, B. Safarzadeh²⁴, M. Zeinali²³

INFN Sezione di Bari ^a, Università di Bari ^b, Politecnico di Bari ^c, Bari, Italy

M. Abbrescia^{a,b}, L. Barbone^{a,b}, C. Calabria^{a,b,5}, S.S. Chhibra^{a,b}, A. Colaleo^a, D. Creanza^{a,c}, N. De Filippis^{a,c,5}, M. De Palma^{a,b}, L. Fiore^a, G. Iaselli^{a,c}, L. Lusito^{a,b}, G. Maggi^{a,c}, M. Maggi^a, B. Marangelli^{a,b}, S. My^{a,c}, S. Nuzzo^{a,b}, N. Pacifico^{a,b}, A. Pompili^{a,b}, G. Pugliese^{a,c}, G. Selvaggi^{a,b}, L. Silvestris^a, G. Singh^{a,b}, R. Venditti, G. Zito^a

INFN Sezione di Bologna ^a, Università di Bologna ^b, Bologna, Italy

G. Abbiendi^a, A.C. Benvenuti^a, D. Bonacorsi^{a,b}, S. Braibant-Giacomelli^{a,b}, L. Brigliadori^{a,b}, P. Capiluppi^{a,b}, A. Castro^{a,b}, F.R. Cavallo^a, M. Cuffiani^{a,b}, G.M. Dallavalle^a, F. Fabbri^a, A. Fanfani^{a,b}, D. Fasanella^{a,b,5}, P. Giacomelli^a, C. Grandi^a, L. Guiducci^{a,b}, S. Marcellini^a, G. Masetti^a, M. Meneghelli^{a,b,5}, A. Montanari^a, F.L. Navarria^{a,b}, F. Odorici^a, A. Perrotta^a, F. Primavera^{a,b}, A.M. Rossi^{a,b}, T. Rovelli^{a,b}, G. Siroli^{a,b}, R. Travaglini^{a,b}

INFN Sezione di Catania ^a, Università di Catania ^b, Catania, Italy

S. Albergo^{a,b}, G. Cappello^{a,b}, M. Chiorboli^{a,b}, S. Costa^{a,b}, R. Potenza^{a,b}, A. Tricomi^{a,b}, C. Tuve^{a,b}

INFN Sezione di Firenze ^a, Università di Firenze ^b, Firenze, Italy

G. Barbagli^a, V. Ciulli^{a,b}, C. Civinini^a, R. D'Alessandro^{a,b}, E. Focardi^{a,b}, S. Frosali^{a,b}, E. Gallo^a, S. Gonzi^{a,b}, M. Meschini^a, S. Paoletti^a, G. Sguazzoni^a, A. Tropiano^{a,5}

INFN Laboratori Nazionali di Frascati, Frascati, Italy

L. Benussi, S. Bianco, S. Colafranceschi²⁵, F. Fabbri, D. Piccolo

INFN Sezione di Genova, Genova, Italy

P. Fabbriatore, R. Musenich

INFN Sezione di Milano-Bicocca ^a, Università di Milano-Bicocca ^b, Milano, Italy

A. Benaglia^{a,b,5}, F. De Guio^{a,b}, L. Di Matteo^{a,b,5}, S. Fiorendi^{a,b}, S. Gennai^{a,5}, A. Ghezzi^{a,b}, S. Malvezzi^a, R.A. Manzoni^{a,b}, A. Martelli^{a,b}, A. Massironi^{a,b,5}, D. Menasce^a, L. Moroni^a, M. Paganoni^{a,b}, D. Pedrini^a, S. Ragazzi^{a,b}, N. Redaelli^a, S. Sala^a, T. Tabarelli de Fatis^{a,b}

INFN Sezione di Napoli ^a, Università di Napoli "Federico II" ^b, Napoli, Italy

S. Buontempo^a, C.A. Carrillo Montoya^{a,5}, N. Cavallo^{a,26}, A. De Cosa^{a,b,5}, O. Dogangun^{a,b}, F. Fabozzi^{a,26}, A.O.M. Iorio^a, L. Lista^a, S. Meola^{a,27}, M. Merola^{a,b}, P. Paolucci^{a,5}

INFN Sezione di Padova ^a, Università di Padova ^b, Università di Trento (Trento) ^c, Padova, Italy

P. Azzi^a, N. Bacchetta^{a,5}, D. Bisello^{a,b}, A. Branca^{a,5}, R. Carlin^{a,b}, P. Checchia^a, T. Dorigo^a, U. Dosselli^a, F. Gasparini^{a,b}, U. Gasparini^{a,b}, A. Gozzelino^a, K. Kanishchev^{a,c}, S. Lacaprara^a, I. Lazzizzera^{a,c}, M. Margoni^{a,b}, A.T. Meneguzzo^{a,b}, J. Pazzini^a, N. Pozzobon^{a,b}, P. Ronchese^{a,b}, F. Simonetto^{a,b}, E. Torassa^a, M. Tosi^{a,b,5}, S. Vanini^{a,b}, P. Zotto^{a,b}, G. Zumerle^{a,b}

INFN Sezione di Pavia ^a, Università di Pavia ^b, Pavia, Italy

M. Gabusi^{a,b}, S.P. Ratti^{a,b}, C. Riccardi^{a,b}, P. Torre^{a,b}, P. Vitulo^{a,b}

INFN Sezione di Perugia ^a, Università di Perugia ^b, Perugia, Italy

M. Biasini^{a,b}, G.M. Bilei^a, L. Fanò^{a,b}, P. Lariccia^{a,b}, A. Lucaroni^{a,b,5}, G. Mantovani^{a,b}, M. Menichelli^a, A. Nappi^{a,b}, F. Romeo^{a,b}, A. Saha^a, A. Santocchia^{a,b}, S. Taroni^{a,b,5}

INFN Sezione di Pisa ^a, Università di Pisa ^b, Scuola Normale Superiore di Pisa ^c, Pisa, Italy

P. Azzurri^{a,c}, G. Bagliesi^a, T. Boccali^a, G. Broccolo^{a,c}, R. Castaldi^a, R.T. D'Agnolo^{a,c}, R. Dell'Orso^a, F. Fiori^{a,b,5}, L. Foà^{a,c}, A. Giassi^a, A. Kraan^a, F. Ligabue^{a,c}, T. Lomtadze^a, L. Martini^{a,28}, A. Messineo^{a,b}, F. Palla^a, A. Rizzi^{a,b}, A.T. Serban^{a,29}, P. Spagnolo^a, P. Squillacioti^{a,5}, R. Tenchini^a, G. Tonelli^{a,b,5}, A. Venturi^{a,5}, P.G. Verdini^a

INFN Sezione di Roma ^a, Università di Roma "La Sapienza" ^b, Roma, Italy

L. Barone^{a,b}, F. Cavallari^a, D. Del Re^{a,b,5}, M. Diemoz^a, M. Grassi^{a,b,5}, E. Longo^{a,b}, P. Meridiani^{a,5}, F. Micheli^{a,b}, S. Nourbakhsh^{a,b}, G. Organtini^{a,b}, R. Paramatti^a, S. Rahatlou^{a,b}, M. Sigamani^a, L. Soffi^{a,b}

INFN Sezione di Torino ^a, Università di Torino ^b, Università del Piemonte Orientale (Novara) ^c, Torino, Italy

N. Amapane^{a,b}, R. Arcidiacono^{a,c}, S. Argiro^{a,b}, M. Arneodo^{a,c}, C. Biino^a, N. Cartiglia^a, M. Costa^{a,b}, N. Demaria^a, C. Mariotti^{a,5}, S. Maselli^a, E. Migliore^{a,b}, V. Monaco^{a,b}, M. Musich^{a,5}, M.M. Obertino^{a,c}, N. Pastrone^a, M. Pelliccioni^a, A. Potenza^{a,b}, A. Romero^{a,b}, M. Ruspa^{a,c}, R. Sacchi^{a,b}, A. Solano^{a,b}, A. Staiano^a, A. Vilela Pereira^a

INFN Sezione di Trieste ^a, Università di Trieste ^b, Trieste, Italy

S. Belforte^a, V. Candelise^{a,b}, F. Cossutti^a, G. Della Ricca^{a,b}, B. Gobbo^a, M. Marone^{a,b,5}, D. Montanino^{a,b,5}, A. Penzo^a, A. Schizzi^{a,b}

Kangwon National University, Chunchon, Korea

S.G. Heo, T.Y. Kim, S.K. Nam

Kyungpook National University, Daegu, Korea

S. Chang, D.H. Kim, G.N. Kim, D.J. Kong, H. Park, S.R. Ro, D.C. Son, T. Son

Chonnam National University, Institute for Universe and Elementary Particles, Kwangju, Korea

J.Y. Kim, Zero J. Kim, S. Song

Korea University, Seoul, Korea

S. Choi, D. Gyun, B. Hong, M. Jo, H. Kim, T.J. Kim, K.S. Lee, D.H. Moon, S.K. Park

University of Seoul, Seoul, Korea

M. Choi, J.H. Kim, C. Park, I.C. Park, S. Park, G. Ryu

Sungkyunkwan University, Suwon, Korea

Y. Cho, Y. Choi, Y.K. Choi, J. Goh, M.S. Kim, E. Kwon, B. Lee, J. Lee, S. Lee, H. Seo, I. Yu

Vilnius University, Vilnius, Lithuania

M.J. Bilinskas, I. Grigelionis, M. Janulis, A. Juodagalvis

Centro de Investigacion y de Estudios Avanzados del IPN, Mexico City, Mexico

H. Castilla-Valdez, E. De La Cruz-Burelo, I. Heredia-de La Cruz, R. Lopez-Fernandez, R. Magaña Villalba, J. Martínez-Ortega, A. Sánchez-Hernández, L.M. Villasenor-Cendejas

Universidad Iberoamericana, Mexico City, Mexico

S. Carrillo Moreno, F. Vazquez Valencia

Benemerita Universidad Autonoma de Puebla, Puebla, Mexico

H.A. Salazar Ibarguen

Universidad Autónoma de San Luis Potosí, San Luis Potosí, Mexico

E. Casimiro Linares, A. Morelos Pineda, M.A. Reyes-Santos

University of Auckland, Auckland, New Zealand

D. Krofcheck

University of Canterbury, Christchurch, New Zealand

A.J. Bell, P.H. Butler, R. Doesburg, S. Reucroft, H. Silverwood

National Centre for Physics, Quaid-I-Azam University, Islamabad, Pakistan

M. Ahmad, M.I. Asghar, H.R. Hoorani, S. Khalid, W.A. Khan, T. Khurshid, S. Qazi, M.A. Shah, M. Shoaib

Institute of Experimental Physics, Faculty of Physics, University of Warsaw, Warsaw, Poland

G. Brona, K. Bunkowski, M. Cwiok, W. Dominik, K. Doroba, A. Kalinowski, M. Konecki, J. Krolikowski

Soltan Institute for Nuclear Studies, Warsaw, Poland

H. Bialkowska, B. Boimska, T. Frueboes, R. Gokieli, M. Górski, M. Kazana, K. Nawrocki, K. Romanowska-Rybinska, M. Szleper, G. Wrochna, P. Zalewski

Laboratório de Instrumentação e Física Experimental de Partículas, Lisboa, Portugal

N. Almeida, P. Bargassa, A. David, P. Faccioli, P.G. Ferreira Parracho, M. Gallinaro, J. Seixas, J. Varela, P. Vischia

Joint Institute for Nuclear Research, Dubna, Russia

P. Bunin, I. Golutvin, I. Gorbunov, A. Kamenev, V. Karjavin, V. Konoplyanikov, G. Kozlov, A. Lanev, A. Malakhov, P. Moisenz, V. Palichik, V. Pereygin, M. Savina, S. Shmatov, V. Smirnov, A. Volodko, A. Zarubin

Petersburg Nuclear Physics Institute, Gatchina (St Petersburg), Russia

S. Evstyukhin, V. Golovtsov, Y. Ivanov, V. Kim, P. Levchenko, V. Murzin, V. Oreshkin, I. Smirnov, V. Sulimov, L. Uvarov, S. Vavilov, A. Vorobyev, An. Vorobyev

Institute for Nuclear Research, Moscow, Russia

Yu. Andreev, A. Dermenev, S. Gninenko, N. Golubev, M. Kirsanov, N. Krasnikov, V. Matveev, A. Pashenkov, D. Tlisov, A. Toropin

Institute for Theoretical and Experimental Physics, Moscow, Russia

V. Epshteyn, M. Erofeeva, V. Gavrilo, M. Kossov⁵, N. Lychkovskaya, V. Popov, G. Safronov, S. Semenov, V. Stolin, E. Vlasov, A. Zhokin

Moscow State University, Moscow, Russia

A. Belyaev, E. Boos, M. Dubinin⁴, L. Dudko, A. Ershov, A. Gribushin, V. Klyukhin, O. Kodolova, I. Lokhtin, A. Markina, S. Obraztsov, M. Perfilov, S. Petrushanko, A. Popov, L. Sarycheva[†], V. Savrin, A. Snigirev

P.N. Lebedev Physical Institute, Moscow, Russia

V. Andreev, M. Azarkin, I. Dremin, M. Kirakosyan, A. Leonidov, G. Mesyats, S.V. Rusakov, A. Vinogradov

State Research Center of Russian Federation, Institute for High Energy Physics, Protvino, Russia

I. Azhgirey, I. Bayshev, S. Bitioukov, V. Grishin⁵, V. Kachanov, D. Konstantinov, A. Korablev, V. Krychkin, V. Petrov, R. Ryutin, A. Sobol, L. Tourtchanovitch, S. Troshin, N. Tyurin, A. Uzunian, A. Volkov

University of Belgrade, Faculty of Physics and Vinca Institute of Nuclear Sciences, Belgrade, Serbia

P. Adzic³⁰, M. Djordjevic, M. Ekmedzic, D. Krpic³⁰, J. Milosevic

Centro de Investigaciones Energéticas Medioambientales y Tecnológicas (CIEMAT), Madrid, Spain

M. Aguilar-Benitez, J. Alcaraz Maestre, P. Arce, C. Battilana, E. Calvo, M. Cerrada, M. Chamizo Llatas, N. Colino, B. De La Cruz, A. Delgado Peris, D. Domínguez Vázquez, C. Fernandez Bedoya, J.P. Fernández Ramos, A. Ferrando, J. Flix, M.C. Fouz, P. Garcia-Abia, O. Gonzalez Lopez, S. Goy Lopez, J.M. Hernandez, M.I. Josa, G. Merino, J. Puerta Pelayo, A. Quintario Olmeda, I. Redondo, L. Romero, J. Santaolalla, M.S. Soares, C. Willmott

Universidad Autónoma de Madrid, Madrid, Spain

C. Albajar, G. Codispoti, J.F. de Trocóniz

Universidad de Oviedo, Oviedo, Spain

H. Brun, J. Cuevas, J. Fernandez Menendez, S. Folgueras, I. Gonzalez Caballero, L. Lloret Iglesias, J. Piedra Gomez³¹

Instituto de Física de Cantabria (IFCA), CSIC-Universidad de Cantabria, Santander, Spain

J.A. Brochero Cifuentes, I.J. Cabrillo, A. Calderon, S.H. Chuang, J. Duarte Campderros, M. Felcini³², M. Fernandez, G. Gomez, J. Gonzalez Sanchez, A. Graziano, C. Jorda, A. Lopez Virto, J. Marco, R. Marco, C. Martinez Rivero, F. Matorras, F.J. Munoz Sanchez, T. Rodrigo, A.Y. Rodríguez-Marrero, A. Ruiz-Jimeno, L. Scodellaro, M. Sobron Sanudo, I. Vila, R. Vilar Cortabitarte

CERN, European Organization for Nuclear Research, Geneva, Switzerland

D. Abbaneo, E. Auffray, G. Auzinger, P. Baillon, A.H. Ball, D. Barney, J.F. Benitez, C. Bernet⁶, G. Bianchi, P. Bloch, A. Bocci, A. Bonato, C. Botta, H. Breuker, T. Camporesi, G. Cerminara, T. Christiansen, J.A. Coarasa Perez, D. D'Enterria, A. Dabrowski, A. De Roeck, S. Di Guida, M. Dobson, N. Dupont-Sagorin, A. Elliott-Peisert, B. Frisch, W. Funk, G. Georgiou, M. Giffels, D. Gigi, K. Gill, D. Giordano, M. Giunta, F. Glege, R. Gomez-Reino Garrido, P. Govoni, S. Gowdy, R. Guida, M. Hansen, P. Harris, C. Hartl, J. Harvey, B. Hegner, A. Hinzmann, V. Innocente, P. Janot, K. Kaadze, E. Karavakis, K. Kousouris, P. Lecoq, Y.-J. Lee, P. Lenzi, C. Lourenço, T. Mäki, M. Malberti, L. Malgeri, M. Mannelli, L. Masetti, F. Meijers, S. Mersi, E. Meschi, R. Moser, M.U. Mozer, M. Mulders, P. Musella, E. Nesvold, T. Orimoto, L. Orsini, E. Palencia Cortezon, E. Perez, L. Perrozzi, A. Petrilli, A. Pfeiffer, M. Pierini, M. Pimiä, D. Piparo, G. Polese, L. Quertenmont,

A. Racz, W. Reece, J. Rodrigues Antunes, G. Rolandi³³, T. Rommerskirchen, C. Rovelli³⁴, M. Rovere, H. Sakulin, F. Santanastasio, C. Schäfer, C. Schwick, I. Segoni, S. Sekmen, A. Sharma, P. Siegrist, P. Silva, M. Simon, P. Sphicas³⁵, D. Spiga, A. Tsirou, G.I. Veres¹⁹, J.R. Vlimant, H.K. Wöhri, S.D. Worm³⁶, W.D. Zeuner

Paul Scherrer Institut, Villigen, Switzerland

W. Bertl, K. Deiters, W. Erdmann, K. Gabathuler, R. Horisberger, Q. Ingram, H.C. Kaestli, S. König, D. Kotlinski, U. Langenegger, F. Meier, D. Renker, T. Rohe, J. Sibille³⁷

Institute for Particle Physics, ETH Zurich, Zurich, Switzerland

L. Bäni, P. Bortignon, M.A. Buchmann, B. Casal, N. Chanon, A. Deisher, G. Dissertori, M. Dittmar, M. Dünser, J. Eugster, K. Freudenreich, C. Grab, D. Hits, P. Lecomte, W. Lustermann, A.C. Marini, P. Martinez Ruiz del Arbol, N. Mohr, F. Moortgat, C. Nägeli³⁸, P. Nef, F. Nessi-Tedaldi, F. Pandolfi, L. Pape, F. Pauss, M. Peruzzi, F.J. Ronga, M. Rossini, L. Sala, A.K. Sanchez, A. Starodumov³⁹, B. Stieger, M. Takahashi, L. Tauscher[†], A. Thea, K. Theofilatos, D. Treille, C. Urscheler, R. Wallny, H.A. Weber, L. Wehrli

Universität Zürich, Zurich, Switzerland

C. Amsler, V. Chiochia, S. De Visscher, C. Favaro, M. Ivova Rikova, B. Millan Mejias, P. Otiougova, P. Robmann, H. Snoek, S. Tupper, M. Verzetti

National Central University, Chung-Li, Taiwan

Y.H. Chang, K.H. Chen, C.M. Kuo, S.W. Li, W. Lin, Z.K. Liu, Y.J. Lu, D. Mekterovic, A.P. Singh, R. Volpe, S.S. Yu

National Taiwan University (NTU), Taipei, Taiwan

P. Bartalini, P. Chang, Y.H. Chang, Y.W. Chang, Y. Chao, K.F. Chen, C. Dietz, U. Grundler, W.-S. Hou, Y. Hsiung, K.Y. Kao, Y.J. Lei, R.-S. Lu, D. Majumder, E. Petrakou, X. Shi, J.G. Shiu, Y.M. Tzeng, X. Wan, M. Wang

Cukurova University, Adana, Turkey

A. Adiguzel, M.N. Bakirci⁴⁰, S. Cerci⁴¹, C. Dozen, I. Dumanoglu, E. Eskut, S. Girgis, G. Gokbulut, E. Gurbinar, I. Hos, E.E. Kangal, T. Karaman, G. Karapinar⁴², A. Kayis Topaksu, G. Onengut, K. Ozdemir, S. Ozturk⁴³, A. Polatoz, K. Sogut⁴⁴, D. Sunar Cerci⁴¹, B. Tali⁴¹, H. Topakli⁴⁰, L.N. Vergili, M. Vergili

Middle East Technical University, Physics Department, Ankara, Turkey

I.V. Akin, T. Aliev, B. Bilin, S. Bilmis, M. Deniz, H. Gamsizkan, A.M. Guler, K. Ocalan, A. Ozpineci, M. Serin, R. Sever, U.E. Surat, M. Yalvac, E. Yildirim, M. Zeyrek

Bogazici University, Istanbul, Turkey

E. Gülmez, B. Isildak⁴⁵, M. Kaya⁴⁶, O. Kaya⁴⁶, S. Ozkorucuklu⁴⁷, N. Sonmez⁴⁸

Istanbul Technical University, Istanbul, Turkey

K. Cankocak

**National Scientific Center, Kharkov Institute of Physics and Technology,
Kharkov, Ukraine**

L. Levchuk

University of Bristol, Bristol, United Kingdom

F. Bostock, J.J. Brooke, E. Clement, D. Cussans, H. Flacher, R. Frazier, J. Goldstein, M. Grimes, G.P. Heath, H.F. Heath, L. Kreczko, S. Metson, D.M. Newbold³⁶, K. Nirunpong, A. Poll, S. Senkin, V.J. Smith, T. Williams

Rutherford Appleton Laboratory, Didcot, United Kingdom

L. Basso⁴⁹, K.W. Bell, A. Belyaev⁴⁹, C. Brew, R.M. Brown, D.J.A. Cockerill, J.A. Coughlan, K. Harder, S. Harper, J. Jackson, B.W. Kennedy, E. Olaiya, D. Petyt, B.C. Radburn-Smith, C.H. Shepherd-Themistocleous, I.R. Tomalin, W.J. Womersley

Imperial College, London, United Kingdom

R. Bainbridge, G. Ball, R. Beuselinck, O. Buchmuller, D. Colling, N. Cripps, M. Cutajar, P. Dauncey, G. Davies, M. Della Negra, W. Ferguson, J. Fulcher, D. Futyan, A. Gilbert, A. Guneratne Bryer, G. Hall, Z. Hatherell, J. Hays, G. Iles, M. Jarvis, G. Karapostoli, L. Lyons, A.-M. Magnan, J. Marrouche, B. Mathias, R. Nandi, J. Nash, A. Nikitenko³⁹, A. Papageorgiou, J. Pela⁵, M. Pesaresi, K. Petridis, M. Pioppi⁵⁰, D.M. Raymond, S. Rogerson, A. Rose, M.J. Ryan, C. Seez, P. Sharp[†], A. Sparrow, M. Stoye, A. Tapper, M. Vazquez Acosta, T. Virdee, S. Wakefield, N. Wardle, T. Whyntie

Brunel University, Uxbridge, United Kingdom

M. Chadwick, J.E. Cole, P.R. Hobson, A. Khan, P. Kyberd, D. Leggat, D. Leslie, W. Martin, I.D. Reid, P. Symonds, L. Teodorescu, M. Turner

Baylor University, Waco, USA

K. Hatakeyama, H. Liu, T. Scarborough

The University of Alabama, Tuscaloosa, USA

O. Charaf, C. Henderson, P. Rumerio

Boston University, Boston, USA

A. Avetisyan, T. Bose, C. Fantasia, A. Heister, J. St. John, P. Lawson, D. Lazic, J. Rohlf, D. Sperka, L. Sulak

Brown University, Providence, USA

J. Alimena, S. Bhattacharya, D. Cutts, A. Ferapontov, U. Heintz, S. Jabeen, G. Kukartsev, E. Laird, G. Landsberg, M. Luk, M. Narain, D. Nguyen, M. Segala, T. Sinthuprasith, T. Speer, K.V. Tsang

University of California, Davis, Davis, USA

R. Breedon, G. Breto, M. Calderon De La Barca Sanchez, S. Chauhan, M. Chertok, J. Conway, R. Conway, P.T. Cox, J. Dolen, R. Erbacher, M. Gardner, R. Houtz, W. Ko, A. Kopecky, R. Lander, T. Miceli, D. Pellett, B. Rutherford, M. Searle, J. Smith, M. Squires, M. Tripathi, R. Vasquez Sierra

University of California, Los Angeles, Los Angeles, USA

V. Andreev, D. Cline, R. Cousins, J. Duris, S. Erhan, P. Everaerts, C. Farrell, J. Hauser, M. Ignatenko, C. Jarvis, C. Plager, G. Rakness, P. Schlein[†], J. Tucker, V. Valuev, M. Weber

University of California, Riverside, Riverside, USA

J. Babb, R. Clare, M.E. Dinardo, J. Ellison, J.W. Gary, F. Giordano, G. Hanson, G.Y. Jeng⁵¹, H. Liu, O.R. Long, A. Luthra, H. Nguyen, S. Paramesvaran, J. Sturdy, S. Sumowidagdo, R. Wilken, S. Wimpenny

University of California, San Diego, La Jolla, USA

W. Andrews, J.G. Branson, G.B. Cerati, S. Cittolin, D. Evans, F. Golf, A. Holzner, R. Kelley, M. Lebourgeois, J. Letts, I. Macneill, B. Mangano, S. Padhi, C. Palmer, G. Petrucciani, M. Pieri, M. Sani, V. Sharma, S. Simon, E. Sudano, M. Tadel, Y. Tu, A. Vartak, S. Wasserbaech⁵², F. Würthwein, A. Yagil, J. Yoo

University of California, Santa Barbara, Santa Barbara, USA

D. Barge, R. Bellan, C. Campagnari, M. D'Alfonso, T. Danielson, K. Flowers, P. Geffert, J. Incandela, C. Justus, P. Kalavase, S.A. Koay, D. Kovalskyi, V. Krutelyov, S. Lowette, N. Mccoll, V. Pavlunin, F. Rebassoo, J. Ribnik, J. Richman, R. Rossin, D. Stuart, W. To, C. West

California Institute of Technology, Pasadena, USA

A. Apresyan, A. Bornheim, Y. Chen, E. Di Marco, J. Duarte, M. Gataullin, Y. Ma, A. Mott, H.B. Newman, C. Rogan, M. Spiropulu⁴, V. Timciuc, P. Traczyk, J. Veverka, R. Wilkinson, Y. Yang, R.Y. Zhu

Carnegie Mellon University, Pittsburgh, USA

B. Akgun, V. Azzolini, R. Carroll, T. Ferguson, Y. Iiyama, D.W. Jang, Y.F. Liu, M. Paulini, H. Vogel, I. Vorobiev

University of Colorado at Boulder, Boulder, USA

J.P. Cumalat, B.R. Drell, C.J. Edelmaier, W.T. Ford, A. Gaz, B. Heyburn, E. Luiggi Lopez, J.G. Smith, K. Stenson, K.A. Ulmer, S.R. Wagner

Cornell University, Ithaca, USA

J. Alexander, A. Chatterjee, N. Eggert, L.K. Gibbons, B. Heltsley, A. Khukhunaishvili, B. Kreis, N. Mirman, G. Nicolas Kaufman, J.R. Patterson, A. Ryd, E. Salvati, W. Sun, W.D. Teo, J. Thom, J. Thompson, J. Vaughan, Y. Weng, L. Winstrom, P. Wittich

Fairfield University, Fairfield, USA

D. Winn

Fermi National Accelerator Laboratory, Batavia, USA

S. Abdullin, M. Albrow, J. Anderson, L.A.T. Bauerdick, A. Beretvas, J. Berryhill, P.C. Bhat, I. Bloch, K. Burkett, J.N. Butler, V. Chetluru, H.W.K. Cheung, F. Chlebana, V.D. Elvira, I. Fisk, J. Freeman, Y. Gao, D. Green, O. Gutsche, J. Hanlon, R.M. Harris, J. Hirschauer, B. Hooberman, S. Jindariani, M. Johnson, U. Joshi, B. Kilminster, B. Klima, S. Kunori, S. Kwan, C. Leonidopoulos, D. Lincoln, R. Lipton, J. Lykken,

K. Maeshima, J.M. Marraffino, S. Maruyama, D. Mason, P. McBride, K. Mishra, S. Mrenna, Y. Musienko⁵³, C. Newman-Holmes, V. O'Dell, O. Prokofyev, E. Sexton-Kennedy, S. Sharma, W.J. Spalding, L. Spiegel, P. Tan, L. Taylor, S. Tkaczyk, N.V. Tran, L. Uplegger, E.W. Vaandering, R. Vidal, J. Whitmore, W. Wu, F. Yang, F. Yumiceva, J.C. Yun

University of Florida, Gainesville, USA

D. Acosta, P. Avery, D. Bourilkov, M. Chen, T. Cheng, S. Das, M. De Gruttola, G.P. Di Giovanni, D. Dobur, A. Drozdetskiy, R.D. Field, M. Fisher, Y. Fu, I.K. Furic, J. Gartner, J. Hugon, B. Kim, J. Konigsberg, A. Korytov, A. Kropivnitskaya, T. Kypreos, J.F. Low, K. Matchev, P. Milenovic⁵⁴, G. Mitselmakher, L. Muniz, R. Remington, A. Rinkevicius, P. Sellers, N. Skhirtladze, M. Snowball, J. Yelton, M. Zakaria

Florida International University, Miami, USA

V. Gaultney, L.M. Lebolo, S. Linn, P. Markowitz, G. Martinez, J.L. Rodriguez

Florida State University, Tallahassee, USA

T. Adams, A. Askew, J. Bochenek, J. Chen, B. Diamond, S.V. Gleyzer, J. Haas, S. Hagopian, V. Hagopian, M. Jenkins, K.F. Johnson, H. Prosper, V. Veeraraghavan, M. Weinberg

Florida Institute of Technology, Melbourne, USA

M.M. Baarmand, B. Dorney, M. Hohlmann, H. Kalakhety, I. Vodopyanov

University of Illinois at Chicago (UIC), Chicago, USA

M.R. Adams, I.M. Anghel, L. Apanasevich, Y. Bai, V.E. Bazterra, R.R. Betts, I. Bucinskaite, J. Callner, R. Cavanaugh, C. Dragoiu, O. Evdokimov, L. Gauthier, C.E. Gerber, D.J. Hofman, S. Khalatyan, F. Lacroix, M. Malek, C. O'Brien, C. Silkworth, D. Strom, N. Varelas

The University of Iowa, Iowa City, USA

U. Akgun, E.A. Albayrak, B. Bilki⁵⁵, W. Clarida, F. Duru, S. Griffiths, J.-P. Merlo, H. Mermerkaya⁵⁶, A. Mestvirishvili, A. Moeller, J. Nachtman, C.R. Newsom, E. Norbeck, Y. Onel, F. Ozok, S. Sen, E. Tiras, J. Wetzel, T. Yetkin, K. Yi

Johns Hopkins University, Baltimore, USA

B.A. Barnett, B. Blumenfeld, S. Bolognesi, D. Fehling, G. Giurgiu, A.V. Gritsan, Z.J. Guo, G. Hu, P. Maksimovic, S. Rappoccio, M. Swartz, A. Whitbeck

The University of Kansas, Lawrence, USA

P. Baringer, A. Bean, G. Benelli, O. Grachov, R.P. Kenny Iii, M. Murray, D. Noonan, S. Sanders, R. Stringer, G. Tinti, J.S. Wood, V. Zhukova

Kansas State University, Manhattan, USA

A.F. Barfuss, T. Bolton, I. Chakaberia, A. Ivanov, S. Khalil, M. Makouski, Y. Maravin, S. Shrestha, I. Svintradze

Lawrence Livermore National Laboratory, Livermore, USA

J. Gronberg, D. Lange, D. Wright

University of Maryland, College Park, USA

A. Baden, M. Boutemour, B. Calvert, S.C. Eno, J.A. Gomez, N.J. Hadley, R.G. Kellogg, M. Kirn, T. Kolberg, Y. Lu, M. Marionneau, A.C. Mignerey, K. Pedro, A. Peterman, A. Skuja, J. Temple, M.B. Tonjes, S.C. Tonwar, E. Twedt

Massachusetts Institute of Technology, Cambridge, USA

A. Apyan, G. Bauer, J. Bendavid, W. Busza, E. Butz, I.A. Cali, M. Chan, V. Dutta, G. Gomez Ceballos, M. Goncharov, K.A. Hahn, Y. Kim, M. Klute, K. Krajczar⁵⁷, W. Li, P.D. Luckey, T. Ma, S. Nahn, C. Paus, D. Ralph, C. Roland, G. Roland, M. Rudolph, G.S.F. Stephans, F. Stöckli, K. Sumorok, K. Sung, D. Velicanu, E.A. Wenger, R. Wolf, B. Wyslouch, S. Xie, M. Yang, Y. Yilmaz, A.S. Yoon, M. Zanetti

University of Minnesota, Minneapolis, USA

S.I. Cooper, B. Dahmes, A. De Benedetti, G. Franzoni, A. Gude, S.C. Kao, K. Klapoetke, Y. Kubota, J. Mans, N. Pastika, R. Rusack, M. Sasseville, A. Singovsky, N. Tambe, J. Turkewitz

University of Mississippi, University, USA

L.M. Cremaldi, R. Kroeger, L. Perera, R. Rahmat, D.A. Sanders

University of Nebraska-Lincoln, Lincoln, USA

E. Avdeeva, K. Bloom, S. Bose, J. Butt, D.R. Claes, A. Dominguez, M. Eads, J. Keller, I. Kravchenko, J. Lazo-Flores, H. Malbouisson, S. Malik, G.R. Snow

State University of New York at Buffalo, Buffalo, USA

U. Baur, A. Godshalk, I. Iashvili, S. Jain, A. Kharchilava, A. Kumar, S.P. Shipkowski, K. Smith

Northeastern University, Boston, USA

G. Alverson, E. Barberis, D. Baumgartel, M. Chasco, J. Haley, D. Nash, D. Trocino, D. Wood, J. Zhang

Northwestern University, Evanston, USA

A. Anastassov, A. Kubik, N. Mucia, N. Odell, R.A. Ofierzynski, B. Pollack, A. Pozdnyakov, M. Schmitt, S. Stoynev, M. Velasco, S. Won

University of Notre Dame, Notre Dame, USA

L. Antonelli, D. Berry, A. Brinkerhoff, M. Hildreth, C. Jessop, D.J. Karmgard, J. Kolb, K. Lannon, W. Luo, S. Lynch, N. Marinelli, D.M. Morse, T. Pearson, R. Ruchti, J. Slaunwhite, N. Valls, M. Wayne, M. Wolf

The Ohio State University, Columbus, USA

B. Bylsma, L.S. Durkin, C. Hill, R. Hughes, K. Kotov, T.Y. Ling, D. Puigh, M. Rodenburg, C. Vuosalo, G. Williams, B.L. Winer

Princeton University, Princeton, USA

N. Adam, E. Berry, P. Elmer, D. Gerbaudo, V. Halyo, P. Hebda, J. Hegeman, A. Hunt, P. Jindal, D. Lopes Pegna, P. Lujan, D. Marlow, T. Medvedeva, M. Mooney, J. Olsen,

P. Piroué, X. Quan, A. Raval, B. Safdi, H. Saka, D. Stickland, C. Tully, J.S. Werner, A. Zuranski

University of Puerto Rico, Mayaguez, USA

J.G. Acosta, E. Brownson, X.T. Huang, A. Lopez, H. Mendez, S. Oliveros, J.E. Ramirez Vargas, A. Zatserklyaniy

Purdue University, West Lafayette, USA

E. Alagoz, V.E. Barnes, D. Benedetti, G. Bolla, D. Bortoletto, M. De Mattia, A. Everett, Z. Hu, M. Jones, O. Koybasi, M. Kress, A.T. Laasanen, N. Leonardo, V. Maroussov, P. Merkel, D.H. Miller, N. Neumeister, I. Shipsey, D. Silvers, A. Svyatkovskiy, M. Vidal Marono, H.D. Yoo, J. Zablocki, Y. Zheng

Purdue University Calumet, Hammond, USA

S. Guragain, N. Parashar

Rice University, Houston, USA

A. Adair, C. Boulahouache, K.M. Ecklund, F.J.M. Geurts, B.P. Padley, R. Redjimi, J. Roberts, J. Zabel

University of Rochester, Rochester, USA

B. Betchart, A. Bodek, Y.S. Chung, R. Covarelli, P. de Barbaro, R. Demina, Y. Eshaq, A. Garcia-Bellido, P. Goldenzweig, J. Han, A. Harel, D.C. Miner, D. Vishnevskiy, M. Zielinski

The Rockefeller University, New York, USA

A. Bhatti, R. Ciesielski, L. Demortier, K. Goulianos, G. Lungu, S. Malik, C. Mesropian

Rutgers, the State University of New Jersey, Piscataway, USA

S. Arora, A. Barker, J.P. Chou, C. Contreras-Campana, E. Contreras-Campana, D. Duggan, D. Ferencek, Y. Gershtein, R. Gray, E. Halkiadakis, D. Hidas, A. Lath, S. Panwalkar, M. Park, R. Patel, V. Rekovic, J. Robles, K. Rose, S. Salur, S. Schnetzer, C. Seitz, S. Somalwar, R. Stone, S. Thomas

University of Tennessee, Knoxville, USA

G. Cerizza, M. Hollingsworth, S. Spanier, Z.C. Yang, A. York

Texas A&M University, College Station, USA

R. Eusebi, W. Flanagan, J. Gilmore, T. Kamon⁵⁸, V. Khotilovich, R. Montalvo, I. Osipenkov, Y. Pakhotin, A. Perloff, J. Roe, A. Safonov, T. Sakuma, S. Sengupta, I. Suarez, A. Tatarinov, D. Toback

Texas Tech University, Lubbock, USA

N. Akchurin, J. Damgov, P.R. Duderov, C. Jeong, K. Kovitanggoon, S.W. Lee, T. Libeiro, Y. Roh, I. Volobouev

Vanderbilt University, Nashville, USA

E. Appelt, C. Florez, S. Greene, A. Gurrola, W. Johns, C. Johnston, P. Kurt, C. Maguire, A. Melo, P. Sheldon, B. Snook, S. Tuo, J. Velkovska

University of Virginia, Charlottesville, USA

M.W. Arenton, M. Balazs, S. Boutle, B. Cox, B. Francis, J. Goodell, R. Hirosky, A. Ledovskoy, C. Lin, C. Neu, J. Wood, R. Yohay

Wayne State University, Detroit, USA

S. Gollapinni, R. Harr, P.E. Karchin, C. Kottachchi Kankanamge Don, P. Lamichhane, A. Sakharov

University of Wisconsin, Madison, USA

M. Anderson, M. Bachtis, D. Belknap, L. Borrello, D. Carlsmith, M. Cepeda, S. Dasu, L. Gray, K.S. Grogg, M. Grothe, R. Hall-Wilton, M. Herndon, A. Hervé, P. Klabbers, J. Klukas, A. Lanaro, C. Lazaridis, J. Leonard, R. Loveless, A. Mohapatra, I. Ojalvo, F. Palmonari, G.A. Pierro, I. Ross, A. Savin, W.H. Smith, J. Swanson

†: Deceased

- 1: Also at Vienna University of Technology, Vienna, Austria
- 2: Also at National Institute of Chemical Physics and Biophysics, Tallinn, Estonia
- 3: Also at Universidade Federal do ABC, Santo Andre, Brazil
- 4: Also at California Institute of Technology, Pasadena, USA
- 5: Also at CERN, European Organization for Nuclear Research, Geneva, Switzerland
- 6: Also at Laboratoire Leprince-Ringuet, Ecole Polytechnique, IN2P3-CNRS, Palaiseau, France
- 7: Also at Suez Canal University, Suez, Egypt
- 8: Also at Zewail City of Science and Technology, Zewail, Egypt
- 9: Also at Cairo University, Cairo, Egypt
- 10: Also at Fayoum University, El-Fayoum, Egypt
- 11: Also at British University, Cairo, Egypt
- 12: Now at Ain Shams University, Cairo, Egypt
- 13: Also at Soltan Institute for Nuclear Studies, Warsaw, Poland
- 14: Also at Université de Haute-Alsace, Mulhouse, France
- 15: Now at Joint Institute for Nuclear Research, Dubna, Russia
- 16: Also at Moscow State University, Moscow, Russia
- 17: Also at Brandenburg University of Technology, Cottbus, Germany
- 18: Also at Institute of Nuclear Research ATOMKI, Debrecen, Hungary
- 19: Also at Eötvös Loránd University, Budapest, Hungary
- 20: Also at Tata Institute of Fundamental Research - HECR, Mumbai, India
- 21: Also at University of Visva-Bharati, Santiniketan, India
- 22: Also at Sharif University of Technology, Tehran, Iran
- 23: Also at Isfahan University of Technology, Isfahan, Iran
- 24: Also at Plasma Physics Research Center, Science and Research Branch, Islamic Azad University, Teheran, Iran
- 25: Also at Facoltà Ingegneria Università di Roma, Roma, Italy
- 26: Also at Università della Basilicata, Potenza, Italy
- 27: Also at Università degli Studi Guglielmo Marconi, Roma, Italy
- 28: Also at Università degli studi di Siena, Siena, Italy
- 29: Also at University of Bucharest, Faculty of Physics, Bucuresti-Magurele, Romania
- 30: Also at Faculty of Physics of University of Belgrade, Belgrade, Serbia
- 31: Also at University of Florida, Gainesville, USA

- 32: Also at University of California, Los Angeles, Los Angeles, USA
- 33: Also at Scuola Normale e Sezione dell' INFN, Pisa, Italy
- 34: Also at INFN Sezione di Roma; Università di Roma "La Sapienza", Roma, Italy
- 35: Also at University of Athens, Athens, Greece
- 36: Also at Rutherford Appleton Laboratory, Didcot, United Kingdom
- 37: Also at The University of Kansas, Lawrence, USA
- 38: Also at Paul Scherrer Institut, Villigen, Switzerland
- 39: Also at Institute for Theoretical and Experimental Physics, Moscow, Russia
- 40: Also at Gaziosmanpasa University, Tokat, Turkey
- 41: Also at Adiyaman University, Adiyaman, Turkey
- 42: Also at Izmir Institute of Technology, Izmir, Turkey
- 43: Also at The University of Iowa, Iowa City, USA
- 44: Also at Mersin University, Mersin, Turkey
- 45: Also at Ozyegin University, Istanbul, Turkey
- 46: Also at Kafkas University, Kars, Turkey
- 47: Also at Suleyman Demirel University, Isparta, Turkey
- 48: Also at Ege University, Izmir, Turkey
- 49: Also at School of Physics and Astronomy, University of Southampton, Southampton, United Kingdom
- 50: Also at INFN Sezione di Perugia; Università di Perugia, Perugia, Italy
- 51: Also at University of Sydney, Sydney, Australia
- 52: Also at Utah Valley University, Orem, USA
- 53: Also at Institute for Nuclear Research, Moscow, Russia
- 54: Also at University of Belgrade, Faculty of Physics and Vinca Institute of Nuclear Sciences, Belgrade, Serbia
- 55: Also at Argonne National Laboratory, Argonne, USA
- 56: Also at Erzincan University, Erzincan, Turkey
- 57: Also at KFKI Research Institute for Particle and Nuclear Physics, Budapest, Hungary
- 58: Also at Kyungpook National University, Daegu, Korea